

Transcriptional changes induced by bone-specific overexpression of
amphiregulin in transgenic mice

von Sabrina Michaela Porada, geb. Vodermeier

Inaugural-Dissertation zur Erlangung der Doktorwürde
der Tierärztlichen Fakultät
der Ludwig-Maximilians-Universität München

Transcriptional changes induced by bone-specific overexpression of
amphiregulin in transgenic mice

von Sabrina Michaela Porada, geb. Vordermeier
aus München

München 2015

Aus dem Veterinärwissenschaftlichen Department
der Tierärztlichen Fakultät der Ludwig-Maximilians-Universität München

Lehrstuhl für Molekulare Tierzucht und Biotechnologie

Arbeit angefertigt unter der Leitung von

PD Dr. Marlon R. Schneider

Gedruckt mit der Genehmigung der Tierärztlichen Fakultät
der Ludwig-Maximilians-Universität München

Dekan: Univ.-Prof. Dr. Joachim Braun

Berichterstatter: Priv.-Doz. Dr. Marlon Schneider

Korreferent: Prof. Dr. Cornelia Deeg

Tag der Promotion: 31.01.2015

To my beloved family

CONTENTS

I.	INTRODUCTION	1
II.	REVIEW OF THE LITERATURE	3
1.	Bone metabolism and osteoporosis	3
1.1.	Bone development.....	3
1.1.1.	Endochondral and intramembranous ossification	3
1.1.2.	Osteoblasts and osteoclasts	3
1.2.	Osteoporosis and treatment options	4
1.2.1.	PTH	6
1.3.	EGF-Receptor system	6
1.4.	Research for new treatment options	10
2.	Transcriptome studies	11
2.1.	Transgenic mice as model for gene expression analysis.....	11
2.2.	Microarray technology	11
2.3.	Col1(I)-AREG mouse line for gene expression analysis	13
III.	MATERIALS AND METHODS	14
1.	Animals	14
1.1.	Col1(I)-AREG transgenic mice.....	14
1.1.1.	Generation of mouse line	14
1.1.2.	Maintenance of mice	15
2.	Materials	16
2.1.	Machines	16
2.2.	Consumables	16
2.3.	Chemicals	16
2.4.	Kits	17
3.	Methods	18
3.1.	Genotyping of mice	18
3.1.1.	DNA-isolation	18
3.1.2.	PCR	19
3.1.3.	Gel electrophoresis	20
3.2.	Sample collection for transcriptome analysis.....	20
3.3.	Transcriptome analysis.....	21

3.3.1.	RNA isolation.....	21
3.3.2.	Microarray analysis	22
3.3.3.	Statistical and bioinformatical analysis of raw microarray data	23
3.3.4.	Evaluation of array data with GO-analysis	23
3.4.	Quantitative RT-PCR	23
3.4.1.	cDNA synthesis	23
3.4.2.	qRT-PCR.....	24
IV.	RESULTS.....	26
1.	Results of transgenic mice generation	26
1.1.	Confirmation of bone-specific overexpression of AREG and increased bone mass in Col1(I)-AREG mice	26
1.2.	Killing of mice and bone collection	28
1.3.	Body weight	28
2.	Microarray analysis	29
2.1.	RNA quality analysis	29
2.2.	Statistical and bioinformatical analysis of the array data.....	31
2.2.1.	GO Analysis	34
2.2.2.	Differentially expressed genes of the 1 week group	35
2.2.3.	Differentially expressed genes of the 4 weeks group.....	41
2.2.4.	Differentially expressed genes of the 8 weeks group.....	43
2.3.	qRT-PCR results	43
V.	DISCUSSION	45
1.1.	Col1(I)-AREG mouse line for transcriptome analysis.....	45
1.2.	Weight and phenotype of transgenic animals	45
1.3.	Transcriptome analysis.....	46
1.4.	Final considerations.....	52
VI.	ZUSAMMENFASSUNG	54
VII.	SUMMARY.....	56
VIII.	BIBLIOGRAPHY	57
IX.	ADDENDUM.....	74
1.	List of tables.....	74

2.	List of figures	74
3.	Primer sequences.....	75
3.1.	PCR primer sequences	75
3.2.	qRT-PCR primer sequences	75
4.	List of genes.....	76
4.1.	1 week, differentially expressed up-regulated genes	76
4.2.	1 week, differentially expressed, down-regulated genes.....	77
4.3.	4 weeks, differentially expressed up-regulated genes.....	82
4.4.	4 weeks, differentially expressed down-regulated genes	83
X.	ACKNOWLEDGMENT.....	84

ABBREVIATIONS

AREG	amphiregulin
ADP	adenosin diphosphate
AMP	adenosin monophosphate
ATP	adenosin triphosphate
bp	base pairs
BTC	betacellulin
Cbfa1	core-binding factor subunit-alpha 1 (see Runx2)
Cdkn2a	cyclin-dependent kinase inhibitor 2A
Col1	collagen I
DAVID	Database for Annotation, Visualization, and Integrated Discovery
DCSTAMP	dendrocyte expressed seven transmembrane protein
DEPC	diethylpyrocarbonate
Δ CT	delta cycle threshold
E	embryonic day
EDTA	ethylene diamine tetraacetic acid
EGF	epidermal growth factor
EGFR	epidermal growth factor receptor
Enpp1	ectonucleotide pyrophosphatase/phosphodiesterase 1 (see PC-1)
EPGN	epigen
ERBB	member of EGFR-family
EREG	epiregulin
Gapdh	glyceraldehydes-3-phosphate dehydrogenase
HBEGF	heparin-binding EGF-like growth factor
HCG	human chorionic gonadotropin
kb	kilobase
M	molar
Map1b	microtubule-associated protein 1B
MCP1	monocyte chemoattractant protein 1
M-CSF	macrophage-colony-stimulating-factor
MMP9	matrix metalloproteinase 9
μ CT	micro-computed tomography
n.c.	non-coding
OPG	osteoprotegerin
OPN	osteopontin (see Spp1)
Osx	osterix
PC-1	plasma cell membrane glycoprotein 1 (see Enpp1)
PMSG	pregnant mare's serum gonadotropin

pQCT	quantitative computed tomography
Pi	inorganic phosphate
PPi	inorganic pyrophosphate
Prrx	paired-related homeobox
PTH	parathyroid hormone
qRT-PCR	quantitative real-time polymerase chain reaction
RANKL	receptor-activator of nuclear factor (NF)- κ B ligand
RIN	RNA integrity number
RNA-Seq	RNA-Sequencing
RT-PCR	real-time polymerase chain reaction
Runx2	runt-related transcription factor (see Cbfa1)
SOTA	self-organizing-tree-algorithm
Spp1	secreted phosphoprotein 1 (see OPN)
tg	transgenic
TGFA	transforming growth factor α
TGF- β	transforming growth factor β
TIMP	tissue inhibitor of metalloproteinases
TNF α	tumor necrosis factor α
wt	wild-type

I. INTRODUCTION

Osteoporosis is a common disease of postmenopausal women and the elderly. Around 1/3 of all postmenopausal women suffer from osteoporosis due to falling estrogen levels in age. It results in reduced bone mineral density and leads to an increased risk of fractures. Normally, the bone mass of healthy adults is kept constant by a balance between constant bone formation and bone resorption. In patients with osteoporosis this mechanism is impaired, leading to decreased bone mass. As a consequence, life quality for these patients is also impaired. Furthermore, even small accidents are likely to cause fractures, especially of wrist, hip or spine, leading to immobility, while pain in the destabilized bones itself, especially in the spine is the reason for reduced mobility, accelerating bone resorption even more ([HTTP://WWW.IOFBONEHEALTH.ORG/](http://www.iofbonehealth.org/)). Treatment costs are expected to rise even more in the coming years; in Germany alone, the estimated costs in the year 2010 were around 9 billion €, which are estimated to rise up to more than 11 billion € by the year 2025 due to an aging population (SVEDBOM et al., 2013). The medications approved for the prevention and treatment of osteoporosis are divided into the two categories, anti-resorptive and anabolic (JOHN M. EISENBERG CENTER FOR CLINICAL DECISIONS AND COMMUNICATIONS SCIENCE, 2007). Like all medicals there are side effects and additionally, patients often stop their treatment after only one year ([HTTP://WWW.IOFBONEHEALTH.ORG/](http://www.iofbonehealth.org/)). On the one hand, this phenomenon is due to the side effects, but there are also many other factors like complex dosing schemes etc. (HERNLUND et al., 2013).

Given the fact that the population will be aging the coming years and the risk of suffering from osteoporosis will be rising, new and improved treatment options must be developed. To achieve this aim, the complex mechanisms involved in bone homeostasis which are not yet fully understood, have to be examined.

Over the last decade there has been quite a progress in bone metabolism research. Examples include the discovery that the Wnt-pathway influences osteoblast formation (WESTENDORF et al., 2004), or the identification of RANKL and OPG as the main mediators on osteoclastogenesis (NAKAGAWA et al., 1998). There is also accumulating evidence that the epidermal growth factor receptor (EGFR) also

plays an important role in bone metabolism (SCHNEIDER et al., 2009b). It has been known that it participates in many developmental processes like growth, proliferation and differentiation of skeletal tissues (XIAN, 2007) and mediates the anabolic actions of PTH, which is used as the only anabolic agent for osteoporosis treatment (POOLE & REEVE, 2005).

The aim of this study was to examine the effect of bone-specific over-expression of amphiregulin (AREG), a ligand of the EGFR. The *Areg* transcript had been detected by microarray analysis to be up-regulated after intermittent PTH treatment (QIN et al., 2005). Therefore, *Areg* might be one of the genes involved in mediating the anabolic effect of intermittent PTH treatment.

II. REVIEW OF THE LITERATURE

1. Bone metabolism and osteoporosis

1.1. Bone development

1.1.1. Endochondral and intramembranous ossification

The skeleton is the scaffold of our body and is characterized by an enormous complexity as it comprises many differently shaped bones with varying amounts of calcified bone and cartilage. Although it has long been considered a quite static tissue its capability for healing and remodeling is enormous, and it serves as a mineral depot that is able to release its contents quickly on metabolic demand (SOMMERFELDT & RUBIN, 2001). Bone has its origin in three embryonic lineages: the craniofacial skeleton is derived from cranial neural crest cells, the axial skeleton from paraxial mesoderm (somites) and the limb skeleton from lateral plate mesodermal cells (OLSEN et al., 2000).

There are two possible ways of bone development: endochondral and intramembranous ossification. Both ways share the first step of forming a mesenchymal template. Most bones are then built by endochondral ossification, where chondroblasts, derived from mesenchymal cells form a chondral scaffold which will be replaced by calcified bone. Only few bones, as the mandibles, the clavicles and certain bones of the skull (DUCY et al., 2000) are built without this cartilaginous frame and are formed directly on the mesenchymal template by intramembranous ossification.

1.1.2. Osteoblasts and osteoclasts

There are three different cell types which can be distinguished in bone: the bone-destroying osteoclasts, the bone-forming osteoblasts and osteocytes, the final differentiation stage of the osteoblast (SOMMERFELDT & RUBIN, 2001).

Osteoblasts have their origin in mesenchymal stem cells (AUBIN, 1998), while the multinucleated osteoclasts originate from hematopoietic stem cells, their precursors descending from monocytes (FUJIKAWA et al., 1996).

The differentiation of osteoblasts is very complex, requiring several transcription factors and growth factors like CBFA1 / RUNX2 and OSX, the main transcription

factors for osteoblast differentiation (DUCY et al., 2000), and involving different pathways like the Wnt-pathway or the Notch-pathway, for example (LONG, 2012). Osteoblasts synthesize osteoid, an organic matrix consisting mainly of collagen I and to a lesser extent proteoglycans and other proteins like signal molecules, which play an important role in bone homeostasis (SOMMERFELDT & RUBIN, 2001). This primary network will then be mineralized by deposition of mineral crystals, calcium and phosphate, forming hydroxyapatites (TITORENCU et al., 2013), the main components of the mineralized bone matrix. Some of the osteoblasts further differentiate to osteocytes, which become trapped in the mineralized matrix, forming dendrite connections between them which enable cell-to-cell communication (BONEWALD, 2011).

Osteoclasts are multinucleated cells, formed by the fusion of progenitors of monocytes/macrophages (TEITELBAUM, 2000). Certain molecules like M-CSF and RANKL are essential for osteoclastogenesis (FELIX et al., 1990; NAKAGAWA et al., 1998; KARSENTY & WAGNER, 2002), whereas OPG inhibits osteoclastogenesis (SIMONET et al., 1997). It has been shown that the differentiation of the osteoclast to the final stage of the bone-resorbing “expert” requires not only factors secreted mainly (but not exclusively) by osteoblasts but also direct cell-to-cell contact with them and marrow stromal cells (UDAGAWA et al., 1990; TEITELBAUM, 2000). On bone contact, the osteoclast forms a “ruffled” membrane, resorbing calcified bone matrix by secretion of several acidifying molecules (TEITELBAUM & ROSS, 2003).

This interaction between bone-forming and bone-resorbing cells indicates a complex system between constant bone formation and bone resorption. Any disturbances of this balance may lead to severe diseases of the skeletal system, resulting in either increased (osteopetrosis) or decreased bone mass (osteoporosis).

1.2. Osteoporosis and treatment options

„A systemic skeletal disease characterized by low bone mass and microarchitectural deterioration of bone tissue with a consequent increase in bone fragility and susceptibility to fracture” is the internationally agreed definition for osteoporosis (CONFERENCE, 1993; KANIS et al., 2008). This definition captures the main “symptom” of osteoporosis: low bone mass. At first, low bone mass alone does not cause any clinical symptoms, but it results in an increased fracture risk, leading not

only to high treatment costs when fractures occur, but also to an increased mortality, especially for patients who suffer from hip fractures (JOHNELL & KANIS, 2005). Therefore several screening tools have been developed to estimate the fracture risk of patients (RUBIN et al., 2013). On the basis of these tools, fracture risks are estimated and suitable treatment options are applied. Basically, treatment options are available as drugs which can act anti-resorptive (calcium, vitamin D, hormone therapy, bisphosphonates, selective estrogen-receptor modulators, and calcitonin) or anabolics (parathyroid hormone, as “Teriparatide”), or a combination of both (Strontium ranelate, stimulates bone formation and avoids bone resorption) (SAMBROOK & COOPER, 2006). Recently, drugs have been developed that directly affect biological pathways involved in bone metabolism, such as Denosumab, an antibody against RANKL, that thus reduces osteoclast activity, and also antibodies which inhibit sclerostin (a protein synthesized by osteocytes, acting as an inhibitor of the Wnt-signaling pathway), thus having an anabolic effect on osteoblast formation (TELLA & GALLAGHER, 2013). As every patient with a potential risk to develop a fracture due to osteoporosis has to be treated individually, and available drugs have side effects which have to be taken into account, there is a constant search for new treatment options. Bisphosphonates for example, accumulate in the skeleton over time, are eliminated by the kidney, and are known to have side effects in patients with reduced renal function but there can be also unwanted effects on the cardiovascular system (ERIKSEN et al., 2014). With the prospect of aging populations and the fact that an increased fracture risk due to osteoporosis occurs mainly in the elderly (DENNISON et al., 2006), it is a main goal for researchers in this field to decrease this risk and therefore avoid the following costs. Another challenge is to overcome poor patient compliance, which is one of the main problems in osteoporosis treatment (HUYBRECHTS et al., 2006; HERNLUND et al., 2013). Several factors seem to be important, including frequency of dosing, adverse events, relationship between patient-physician, etc. (HERNLUND et al., 2013), whereas simplicity of dosing seems to correlate with better compliance (CLAXTON et al., 2001). The novel agent Denosumab for example, which belongs to a new class of antiresorptives by acting as an antibody, has been proven to effectively increase bone mass density when given in a 6 months interval (BONE et al., 2011). But so far there is only one anabolic agent available for osteoporosis treatment: PTH. The greatest disadvantage of PTH is the need of daily administration (CANALIS, 2010).

1.2.1. PTH

PTH, a 84 amino acid-long peptide hormone, that is secreted by the parathyroid gland, is one of the three main mediators responsible for blood-calcium-homeostasis; the other two are calcitonin and 1,25-dihydroxyvitamin D. Physiologically, PTH has catabolic functions on bone. Decreasing blood calcium levels cause PTH to release calcium from bones by osteoclast stimulation and therefore bone resorption (MUNDY & GUISE, 1999). Interestingly, PTH has quite the reverse effect when given intermittently (GUNNESS-HEY & HOCK, 1984; DOBNIG & TURNER, 1995). This effect is used for the treatment of osteoporosis as described before. “Teriparatide” contains recombinant human PTH (amino acids 1-34 of the N-terminal region of the 84 amino acids long peptide, which is the biological active region) and is used as an anabolic agent for osteoporosis therapy as it stimulates bone formation and increases bone mineral density (NEER et al., 2001; TELLA & GALLAGHER, 2013), therefore reducing fracture risk effectively. It is largely unknown how this effect is mediated. PTH is known to influence the expression of several genes involved in bone homeostasis. For example, the expression of type 1 collagen, alkaline phosphatase, osteonectin (ON) and osteopontin (OPN) are decreased by PTH-stimulation, while the expression of genes like collagenase-3, tissue inhibitors of metalloproteinases (TIMPs), insulin-like growth factor 1 (IGF-1), tissue-type plasminogen activator (tPA), interleukin (IL)-6, and leukemia inhibitory factor are increased (SWARTHOUT et al., 2002). The expression of another potent factor for pre-osteoblast proliferation, fibroblast growth factor 2 (FGF-2) is also increased by PTH (SABBIETI et al., 2009). It could be shown by microarray analysis, that treatment of an osteoblast-like cell line, rat UMR 106-01, with PTH stimulated the expression of another gene: *Areg*, encoding amphiregulin, a ligand of the epidermal growth factor receptor (EGFR) (QIN et al., 2003; QIN & PARTRIDGE, 2005; QIN et al., 2005). On the other hand, mice lacking *Areg* had less trabecular bone than wild-type animals (LUETTEKE et al., 1999; QIN et al., 2005), which leads to the conclusion that the bone anabolic effect of PTH may be greatly influenced by the EGFR-system.

1.3. EGF-Receptor system

The EGFR-system comprises four structurally related receptors, ERBB1 (EGFR), ERBB2, ERBB3 and ERBB4, and seven growth factors that are able to activate the EGFR: epidermal growth factor (EGF), transforming-growth factor α (TGFA),

heparin-binding EGF-like growth factor (HBEGF), betacellulin (BTC), amphiregulin (AREG), epiregulin (EREG) and epigen (EPGN) (YARDEN & SLIWKOWSKI, 2001; HARRIS et al., 2003; SCHNEIDER & WOLF, 2009).

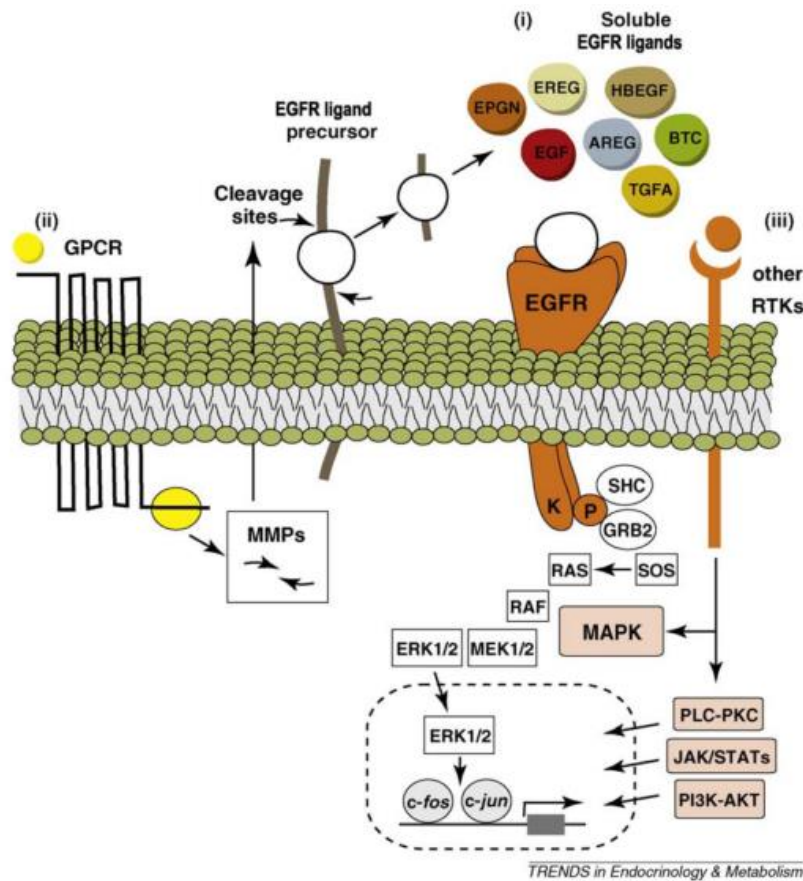


Figure 1: Overview of the EGFR system

Reprinted from Schneider et al., *Trends in Endocrinology and Pathology*, 20, 517-524, (2009) with permission from Elsevier:

- i) Receptor dimers are formed upon ligand binding and initiating intracellular signaling cascades
- ii) Activation of EGFR via heterologous signals: here G-protein-coupled receptors (GPCRs) and
- iii) other receptor tyrosine kinases (RTKs)

These receptors belong to the family of receptor tyrosine kinases, and include an extracellular ligand-binding region, a single membrane-spanning domain, and a cytoplasmic protein tyrosine kinase-containing region which forms homo- or heterodimers after ligand-binding, causing autophosphorylation of the cytoplasmic

tyrosine residues (**Figure 1**) (YARDEN & SLIWKOWSKI, 2001; HOLBRO & HYNES, 2004). These phosphorylated tyrosine residues serve as docking sites for intracellular signal molecules (OLAYIOYE et al., 2000), initiating multiple and complex signaling cascades essential for growth, differentiation, repair and survival of various tissues (ODA et al., 2005; YARDEN & SHILO, 2007).

The ERBB-receptors are required for development, as demonstrated by the generation of mutant mouse lines lacking individual receptors:

The EGFR (ERBB1) is an autonomous receptor, which is able to bind many ligands and form not only heterodimers but also homodimers (CITRI & YARDEN, 2006). EGFR knockout mice viability depends on their genetic background. In a 129/Sv background, mice are not viable and die at midgestation, due to a placental defect (SIBILIA et al., 2003), in a C57BL/6 background they die at birth and in MF1, C3H and CD 1 background some mice can reach an age of 20 days post partum (THREADGILL et al., 1995; SIBILIA et al., 2003). Several severe alterations of their phenotypes were observed, including alterations of the epithelium, the neural system and craniofacial malformations (MIETTINEN et al., 1995; SIBILIA & WAGNER, 1995; THREADGILL et al., 1995; MIETTINEN et al., 1999), leading to the early death of these knockout mice.

Although ERBB2 cannot bind any ligands itself, it functions as the preferred partner for heterodimer-building (TZAHAR et al., 1996; CITRI & YARDEN, 2006). ERBB2 knockout mice die during embryonic development before E11 due to malformations of the heart, resulting in complete absence of heart trabeculae and therefore impaired heart function. Additionally severe alterations of the neural system could be found (LEE et al., 1995).

Like ERBB2, ERBB3 itself is non-autonomous, but forms functional heterodimers with other ERBB-receptors (CITRI & YARDEN, 2006). ERBB3-deficient mice die around E13.5 also due to heart malformations. Those mice have a noticeably thinned heart wall and an insufficient valve function, resulting in blood reflux. In addition, these mice also show a hypoplastic cerebellar region (ERICKSON et al., 1997).

ERBB4 has similarities to ERBB1; it is an autonomous receptor which is able to bind to many ligands (CITRI & YARDEN, 2006). It is highly expressed in heart muscle and certain regions of the nervous system. ERBB4-deficient mice die

around E10.5; like in ERBB2 knockout mice, no heart trabeculae were detectable, leading to an impaired heart function and resulting in early lethality (GASSMANN et al., 1995).

As mentioned above, knockout of the EGFR reduces life expectancy dramatically, and it is essential for the normal development of most tissues (MIETTINEN et al., 1995; SIBILIA & WAGNER, 1995; MIETTINEN et al., 1999). It has been known for a long time that the EGFR-system plays also an important role in bone development, especially in bone formation (CANALIS & RAISZ, 1979; KUMEGAWA et al., 1983; NG et al., 1983; HATA et al., 1984; FANG et al., 1992; LOZA et al., 1995; CHIEN et al., 2000; QIN et al., 2005). Further studies showed that the EGFR promotes proliferation of bone-forming osteoblasts and inhibits their maturation and therefore mineralization of the bone (SIBILIA et al., 2003). On the other hand, transgenic mice overexpressing specific EGFR-ligands exhibit quite different bone phenotypes. Overexpression of EGF, for example, results in a reduced thickness of cortical bone due to accumulation of overproliferated osteoblasts in the endosteum and periosteum (CHAN & WONG, 2000), and mice overexpressing BTC are characterized by a high bone mass of the long bones (SCHNEIDER et al., 2009a). Transgenic mice overexpressing TGFA (JHAPPAN et al., 1990; SANDGREN et al., 1990) or HBEGF (PROVENZANO et al., 2005) on the other hand, showed no alterations of bone. For an overview of the influence of the EGFR network in bone cells see **Figure 2**.

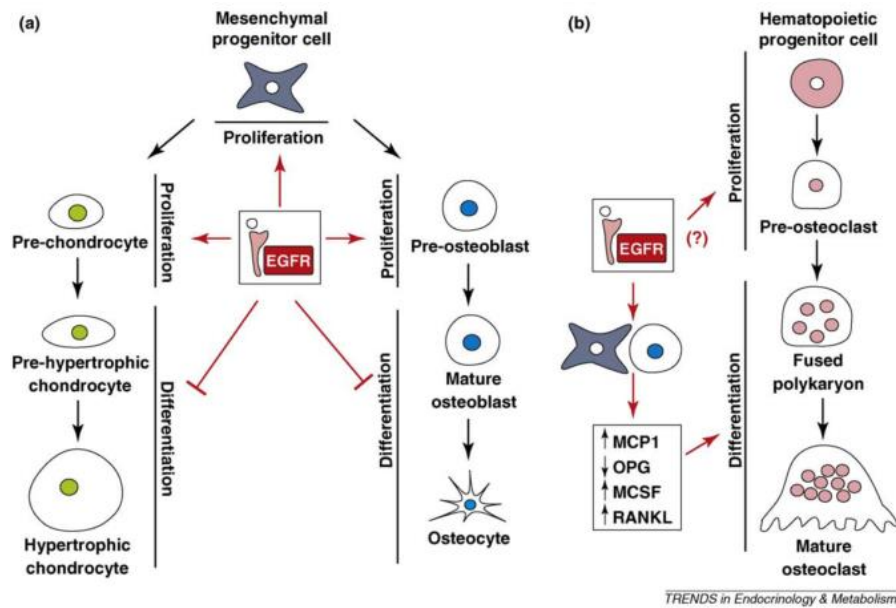


Figure 2: Effect of EGFR network on bone cells

Reprinted from Schneider et al., *Trends in Endocrinology and Pathology*, 20, 517-524, (2009) with permission from Elsevier:

- a) Stimulation of proliferation of pre-chondrocytes and pre-osteoblasts via EGFR and inhibition of final differentiation
- b) Effect on pre-osteoclasts not fully understood, but stimulation of osteoclast differentiation via up-regulation of MCP1, MCSF, RANKL and down-regulation of OPG

1.4. Research for new treatment options

All available agents for the treatment of osteoporosis have side effects. PTH, for example, is approved for osteoporosis treatment for a maximal period of 2 years, due to the development of osteosarcomas in rat studies (MCGREEVY & WILLIAMS, 2011). As the only bone anabolic agent for osteoporosis treatment currently is PTH, and there is still need for novel agents for the treatment of osteoporosis, researchers are focusing on new agents that act through biological pathways with great potential for developing new therapy strategies. For example the Wnt-pathway (CANALIS, 2013), as it has been discovered that an activation of this pathway leads to an increase of bone mass (WESTENDORF et al., 2004). The EGFR-system may be another potential candidate for the development of new therapeutic agents, as its influence on bone homeostasis is quite obvious. *Areg* is a

target gene of the anabolic action of PTH, but how this effect is mediated is still unclear. It might be worth to investigate how AREG influences bone formation. Uncovering the mechanism by which AREG functions on bone formation may lead to the discovery of novel anabolic agents, which could be of use in osteoporosis treatment.

2. Transcriptome studies

2.1. Transgenic mice as model for gene expression analysis

Transgenic animals have been used for decades as suitable models for studying gene functions, interactions of gene products in biological processes or their role in pathological processes (CHO et al., 2009). The method for generating transgenic animals by microinjection of foreign DNA into the pronucleus of fertilized mouse oocytes, which has first been reported more than 30 years ago (GORDON et al., 1980), has become a standard and indispensable tool for scientific research since and can be found in several overviews (CONNER, 2004; CHO et al., 2009; HARUYAMA et al., 2009). Transgenic mouse lines may also be generated with the aim of conducting a transcriptome analysis, which may provide more information about the mechanism behind the observed phenotypes.

2.2. Microarray technology

The successful sequencing of the genome of many organisms was the first step on the way before it became possible to examine differences in expression patterns of genes. Yet, uncovering the sequences of the genome of an organism alone does not yield information about expression patterns or the functions of single genes. The transcribed mRNA is the first step from DNA to protein synthesis. So the transcript of an organism is the imprint of the “currently active” genes, which is, unlike the genome, very dynamic and changes rapidly with outer stimulation or during biological processes (LOCKHART & WINZELER, 2000). The principle behind the microarray technology, a powerful tool for transcriptome analysis, is the same like Northern or Southern blotting: the target sequences are detected by hybridization to a compatible immobilized sequence. An array comprises complementary DNA, obtained by PCR from cDNA libraries, immobilized in high density on a matrix, usually on glass, at defined positions (termed as probe). The mRNA, the transcript of a given cell line or tissue, will then be used to generate a fluorescent labeled “target”, that, in turn, will be hybridized to the compatible

immobilized sequence (SCHENA et al., 1995; SCHULZE & DOWNWARD, 2001). The intensity of bound “target”, measured by the fluorescent intensity, corresponds to the amount of mRNA isolated from the sample. Because of the high density assembly of cDNA on an array, one chip contains many thousands of different cDNA clones, and is therefore an appropriate tool for gene expression monitoring (LOCKHART & WINZELER, 2000).

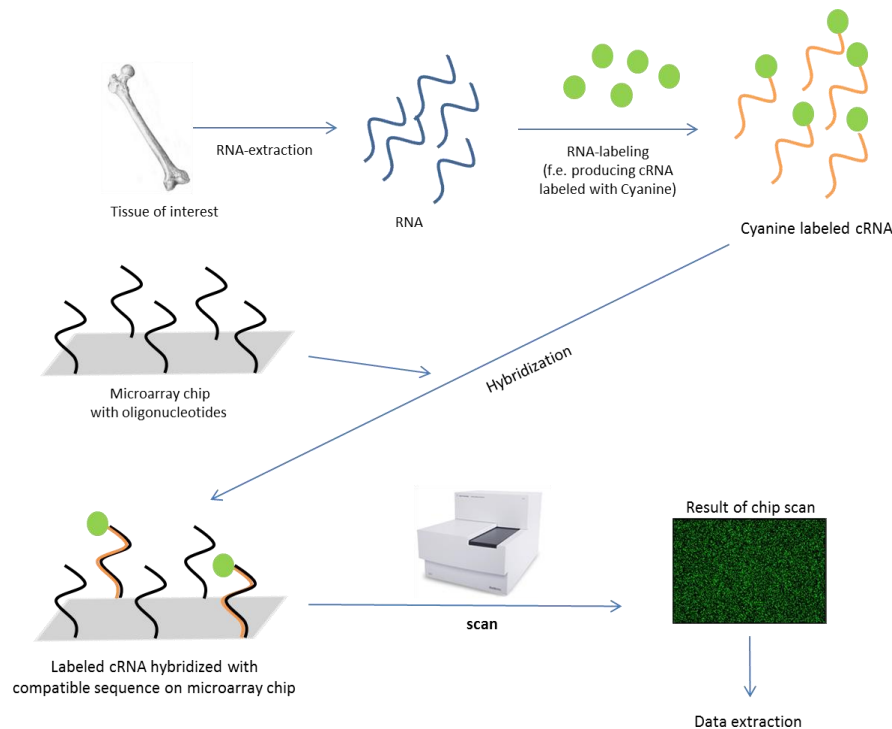


Figure 3: Microarray analysis scheme

For this work, the Agilent SurePrint Mouse GE 8x60K Microarray Kit (Agilent, Waldbronn) was used. According to the manufacturer, this array comprises ~ 39500 Entrez gene RNAs and ~ 16000 linc RNAs, and covers all currently known genes and intergenic, non-coding RNAs ([HTTP://WWW.GENOMICS.AGILENT.COM/EN/HOME.JSP](http://www.genomics.agilent.com/en/home.jsp)).

2.3. Col1(I)-AREG mouse line for gene expression analysis

As the specific pathways responsible for AREG effects on osteoblasts are unknown, we conducted a transcriptome analysis via microarray to identify the genes up- or down-regulated in osteoblasts of Col1(I)-AREG transgenic mice, a mouse line overexpressing AREG specifically in osteoblasts (described below), compared to wild-type controls.

For this work, bones, in this case, whole femurs, were used for the microarray experiment. We chose different age groups to evaluate possible age-related dynamics of the transgene compared to wild-types:

1 week (newborn)

4 weeks (adolescent)

8 weeks (adult)

As sex steroids are also known to influence bone metabolism (RIGGS et al., 2002), we chose only male mice for the experiments.

III. MATERIALS AND METHODS

1. Animals

1.1. Col α 1(I)-AREG transgenic mice

To examine the potential of AREG to increase bone mass in vivo, a mouse line overexpressing AREG specifically in the bone was created in the Gene Center by PD Dr. Marlon Schneider. In this mouse line the *Areg* cDNA is driven by the osteoblast-specific murine 2.3 kb collagen α 1(I) promoter (DACQUIN et al., 2002) to ensure an overexpression only in osteoblasts.

1.1.1. Generation of mouse line

Initially, the *Areg* cDNA (~ 800 bp) was obtained from a mouse skin cDNA library by RT-PCR (Platinum Taq DNA Polymerase High Fidelity System (Invitrogen, Carlsbad) using the following primers:

Areg Xba#1: 5` -TAG TCT AGA TTG CTG CAG AGA CCG AGA C- 3`

(XbaI sequence underlined)

Areg Pac#2: 5` -TAG TTA ATT AAG GCA ATG ATT CAA CTT TTA CC- 3`

(PacI sequence underlined)

The transcript was cloned into the pCRII-TOPO vector and sequenced to confirm amplification fidelity.

The AREG transcript was excised with the restriction enzymes XbaI and PacI. Simultaneously, a 2.3 kb fragment of the mouse α 1(I)-collagen promoter was excised with a XhoI/XbaI double digest from the pJ251 plasmid, a generous gift from G. Karsenty (DACQUIN et al., 2002). The two fragments were then cloned in a single step into a XhoI/PacI – opened Bluescript plasmid, containing a bovine growth hormone polyadenylation signal. The correct assembly was confirmed by multiple restriction enzyme digests and sequencing before the 3.5 kb Coll1 α (I)-AREG transgene was released from the Bluescript plasmid backbone by a NotI digest. Purification of the transcript DNA was performed by an agarose-gel purification method (CHO et al., 2009).

Zygotes for microinjection were obtained from FVB females, which had been

superovulated with PMSG (Intergonan®, Intervet, Unterschleißheim) followed by application of HCG (Ovogest®, Intervet, Unterschleißheim) two days later. After injection of HCG, donors were mated with male FVB mice. The next day females were checked for positive vaginal plugs, the positive ones were killed to collect zygotes for DNA microinjection. The method for DNA microinjection into the male pronucleus was conducted according to standard methods (CONNER, 2004; CHO et al., 2009; HARUYAMA et al., 2009; LIU et al., 2013). The injected zygotes were implanted surgically into NMRI foster mothers, which had been plug positive the same day as the donors. Born pups were genotyped as described below to identify transgenic founders. A total of three positive founders were obtained. Only the lines descending from animal 1 (line1, L1) and animal 3 (line3, L3) were positive for the transgene. Descendants from animal 2 did not carry the transgene.

1.1.2. Maintenance of mice

Mice were maintained under specific pathogen-free conditions in a closed barrier facility with autoclave, personal and material barrier.

Maintenance conditions:

25° Celsius constantly

Humidity 45 %

Overpressure (dynamic, depending on barometric pressure)

Light program: 12 h light cycle, beginning at 7 am, 12 h dark cycle, beginning at 7 pm

Mice were held in Macrolon Cages type II long and type III, weaned and separated by sex at the age of 4 weeks. At the same time mice were earmarked and tail tips were collected for genotyping.

All mice had ad libitum access to a standard rodent diet (V1534, Ssniff, Soest) and water. Additionally, all mice obtained cage enrichment (red houses, cellulose paper, running wheels, etc.) to improve maintenance conditions. All procedures were carried out in accordance with the German Animal Protection Law.

2. Materials

2.1. Machines

Bioanalyzer 2100	Agilent, Waldbronn
Centrifuge (5417R)	Eppendorf, Hamburg
Chyo MJ-3000 (analytical balance)	Chyo, Japan
Homogenizer	Art Miccra, Müllheim
Mastercycler® ep realplex	Eppendorf, Hamburg
PCR machine	
Nanodrop ND-1000	Peqlab Biotechnology, Erlangen
Thermocycler	Biometra®, Göttingen
Thermomixer	Eppendorf, Hamburg

2.2. Consumables

Heat-sealing foils for PCR plates	Eppendorf, Hamburg
Histoacryl® liquid skin glue	B. Braun, Melsungen
QualiPCRTube-strips	Kisher Biotech, Steinfurt
round bottom tubes, 4 ml	Carl Roth GmbH, Karlsruhe
Standard Rodent diet (V1534)	Ssniff, Soest
Safe-lock tubes (1.5 ml)	Eppendorf, Hamburg
96 well real-time PCR plates	Eppendorf, Hamburg

2.3. Chemicals

Agarose	Invitrogen, Karlsruhe
Chloroform	Merck, Darmstadt
DEPC	Sigma, Deisenhofen
DNase I (1U/μl)	Thermo Scientific, St. Leon-Roth

DNA-Rehydration Solution	Promega, Mannheim
dNTPs	Thermo Scientific, St. Leon-Roth
EDTA	VWR, Darmstadt
Ethanol	Carl Roth GmbH, Karlsruhe
Ethidium bromide	Carl Roth GmbH, Karlsruhe
Gene Ruler, 100 bp	Thermo Scientific, St. Leon-Roth
Glacial acetic acid	Carl Roth GmbH, Karlsruhe
HotStar Taq Polymerase	Quiagen, Hilden
Isopropanol	VWR, Darmstadt
Nuclei Lysis Solution	Promega, Mannheim
Protein Precipitation Solution	Promega, Mannheim
Proteinase K (20 mg/mg)	Roche, Mannheim
Random Hexamer Primer	Thermo Scientific, St. Leon-Roth
Reaction Buffer (5x; 10x)	Thermo Scientific, St. Leon-Roth
RevertAid Reverse Transcriptase	Thermo Scientific, St. Leon-Roth
RNAse	Promega, Mannheim
Ribolock RNAse Inhibitor	Thermo Scientific, St. Leon-Roth
SYBR® Green	Lonza, Basel
Tris	Carl Roth GmbH, Karlsruhe
Trizol® Reagent	Life technologies, Carlsbad

2.4. Kits

Agilent RNA Spike-In Kit, One Color, Cat. 5188-5282, Agilent, Waldbronn

Agilent Low-Input QuickAmp Labeling Kit, Cat. 5190-2331, Agilent, Waldbronn

Agilent Cyanine 3 CTP Dye Pack, No. 5188-1169-P, Agilent, Waldbronn

Agilent Gene Expression Hybridization Kit, Cat. 51885242, Agilent, Waldbronn

Agilent Microarray Chip G4852A surePrint Mouse GE 8*60k, Cat. 4852-60510, Agilent, Waldbronn

Platinum Taq DNA Polymerase High Fidelity System, Invitrogen, Carlsbad

Taq DNA polymerase Kit, Quiagen, Hilden

Wizard DNA Purification Kit, Promega, Mannheim

3. Methods

3.1. Genotyping of mice

Mice destined for the 4 weeks and 8 weeks groups were marked by ear punches and tail tip samples for genotyping were collected before sacrifice. A small piece from the end of the tail was cut with a pair of scissors and the wound treated with Histoacryl® liquid skin glue (B. Braun, Melsungen). The animals for the 1 week group were killed and tail tips for genotyping were collected simultaneously. The tail tip samples were immediately frozen on dry ice and stored in a 1.5 ml Eppendorf tube at -80° C before further processing.

3.1.1. DNA-isolation

Tail tip samples were incubated overnight in 1.5 ml safe-lock tubes (Eppendorf, Hamburg) at 56° C, shaking slightly, with 620 µl tissue digestion mix buffer, containing:

500 µl Nuclei Lysis Solution (Promega, Mannheim)

120 µl 0.5 M EDTA pH 8,0

17.5 µl Proteinase K, 20 mg/ml, Roche, Mannheim.

Further processing next day started with adding 3 µl of RNase (Promega, Mannheim) and incubating at 37° C for 20 min, with moderate shaking.

Next, 200 µl of Protein Precipitation Solution (Promega, Mannheim) were added, the tube was vortexed vigorously for 20 s, and then stored on ice for approximately 5 min. After that, the tubes were centrifuged at 20000 x g. After centrifugation, the supernatant, which contained the DNA, was removed carefully without taking the protein pellet from the bottom, and transferred into another 1.5 ml safe-lock tube containing 600 µl isopropanol (VWR, Darmstadt). The DNA precipitated after

inverting the tube gently for several times. Probes were centrifuged again at 20000 x g to obtain a DNA pellet at the bottom of the tube. Isopropanol was poured of carefully and the remaining pellet was washed with 600 µl 70% ethanol (Carl Roth, Karlsruhe). After centrifuging the probes again, ethanol was also poured of, small remnants were removed by a 10 µl pipette and the pellet was air-dried for approximately 10 min. To dissolve the dried pellet, 50 µl of DNA Rehydration Solution (Promega, Mannheim) were added and the tubes either incubated for 1 h at 65° C or stored overnight at +4° C before further processing.

3.1.2. PCR

For PCR the Taq DNA Polymerase Kit, Category 1000 Units (Qiagen, Hilden) and QualiPCRTube-strips, RNase-, DNase- and pyrogen-free (Kisher Biotech, Steinfurt) were used.

For each probe, a mastermix, containing the following components was prepared:

10x CoralLoad Reaction Buffer	2 µl
dNTPs, 1 mM	2 µl
Q-Solution, 5x	4 µl
MgCl ₂	1.25 µl
Primer (sense)	1 µl
Primer (antisense)	1 µl
Bidistilled water	7.65 µl
Taq DNA-polymerase	0.1 µl
DNA-probe	1 µl

Primers were:

Areg Xba#1 (sense primer):

5` TAG TCT AGA TTG CTG CAG AGA CCG AGA C 3`

Areg Pac#2 (antisense primer):

5` TAG TTA ATT AAG GCA ATG ATT CAA CTT TTA CC 3`

Reaction protocol for thermocycler (Biometra®, Göttingen):

3.3. Transcriptome analysis

3.3.1. RNA isolation

For the extraction of RNA from the femurs the Trizol® Reagent protocol was adopted. 1.7 ml Trizol® were added to the frozen femurs and they were immediately homogenized with a Homogenizer (Art Micra, Müllheim) in a 4 ml round bottom tube.

Phase separation:

0.8 ml of the mix were transferred to a new reaction tube and 160 µl chloroform (0.2 ml chloroform/1 ml Trizol) were added and shaken vigorously per hand for 15 s. The mixture was then incubated at room temperature for 10 min, followed by centrifugation for 35 min, 20000 x g at 4° C. A separation of the mixture was now visible: an upper red phenol-chloroform-phase, a cloudy white interphase and a lower clear phase.

Precipitation:

The upper clear phase, which contains the RNA, was removed with a pipette into a new reaction tube and 0.4 ml isopropanol (0.5 ml isopropanol/1 ml Trizol®) were added, vortexed and incubated at room temperature for 10 min. Next the tubes were centrifuged for 45 min, 20000 x g at 4° C to obtain an RNA pellet at the bottom of the tube.

RNA wash:

The supernatant was discarded and the RNA washed with 0.8 ml 75% ethanol (1 ml ethanol/1 ml Trizol®). Next, the tubes were again centrifuged at 25000 x g for 10 min at 4° C. This step was repeated after discarding the supernatant and washing again with 0.4 ml ethanol (0.5 ml ethanol/1 ml Trizol®).

After taking of the supernatant ethanol, the tubes were centrifuged shortly and the remaining ethanol was taken with a pipette. The RNA pellet was dried carefully at the flame of a Bunsen burner for approximately 6 min, till it became clear.

RNA resuspension

70 µl of RNAase-free water was added to the tubes for resuspension and an incubation step followed for 20 min at 35° C on a thermomixer.

Quality of RNA

Quality and concentration of RNA were assessed by Nanodropspectrophotometer and Bioanalyzer. Additionally an agarose gel was run for quality control of RNA. A 260:280 ratio of ~2 is considered “pure” for RNA (Nanodrop). Quality control with Bioanalyzer: RNA integrity number (RIN) was for all samples 8.5 – 10 (10: very good quality of RNA; 1: very poor quality/contaminated RNA)

3.3.2. Microarray analysis

The microarray experiments were kindly conducted by members of the laboratory of Dr. Helmut Blum in the Gene Center.

Before hybridization with the Agilent Microarray Chip (Agilent Gene Expression Hybridization Kit, Agilent, Waldbronn) fluorescent cRNA synthesis with Cyanine3 was conducted with the QuickAmp Labeling Kit, one color (Agilent, Waldbronn) according to the manufacturer’s instructions.

Figure 4 shows a diagram with the steps for Microarray chip hybridization.

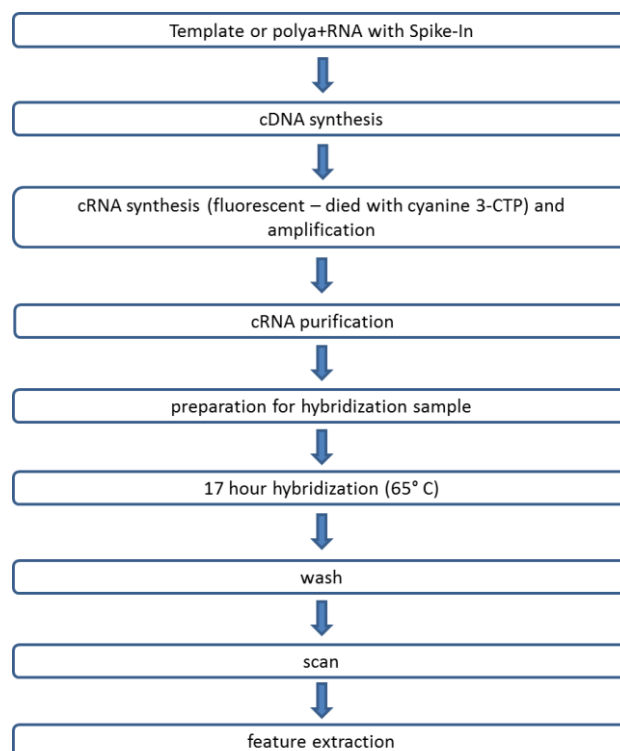


Figure 4: Hybridization process of probe with microarray chip

Modified from Agilent user’s manual for One-Color Microarray-Based Gene Expression Analysis

3.3.3. Statistical and bioinformatical analysis of raw microarray data

The statistical and bioinformatical analysis of the raw Agilent Array data was kindly conducted by Alexander Graf of the laboratory of Dr. Helmut Blum in the Gene Center, Munich.

3.3.4. Evaluation of array data with GO-analysis

The obtained lists of differentially expressed genes were further analyzed with the free online bioinformatics resource DAVID (Database for Annotation, Visualization, and Integrated Discovery) (Version: 6.7) (DENNIS et al., 2003) and the open source bioinformatics network Cytoscape (Version: 3.0.2) (SHANNON et al., 2003). These tools were used to search for overrepresented annotation categories and visualize correlations between the found terms and the selected genes. For the analysis with Cytoscape, the basic settings of the program with the Apps CluGo and CluPedia were used, except for the analysis of the down-regulated genes of the 1 week group. Network specificity was positioned halfway between “medium” and “significant” for this gene list, as the basic setting (positioned near “medium”) yielded no manageable result.

As the overexpressed *Areg*-gene was inserted artificially, it was excluded from the analyzed lists of differentially expressed genes for all age-groups.

3.4. Quantitative RT-PCR

3.4.1. cDNA synthesis

Three samples of the 1 week group and three of the controls were chosen for cDNA synthesis and quantitative RT-PCR. A final amount of 1 µg of RNA was used for cDNA synthesis.

DNase digest

1 µl of 10x Reaction buffer and 1 µl of DNase I (1U/µl) (Thermo Scientific, St. Leon-Roth) were added to each sample in safe lock tubes and incubated for 30 min at 37° C in a thermomixer. After incubation 1 µl of 50 mM EDTA was added to each sample to stop the enzymatic reaction. Another incubation step at 65° C for 10 min followed.

Reverse transcription

First 1 µl of Random Hexamer Primer (Thermo Scientific, St. Leon-Roth) was

pipetted to each sample and an incubation step at 65° C for 5 min followed.

For reverse transcription to each sample was added:

4 µl	5x Reaction Buffer (Thermo Scientific, St. Leon-Roth)
0.5 µl	Ribolock RNase Inhibitor (Thermo Scientific, St. Leon-Roth)
2 µl	dNTPs 10 mM (Thermo Scientific, St. Leon-Roth)
1 µl	RevertAid Reverse Transcriptase (Thermo Scientific, St. Leon-Roth)

Three incubation steps followed:

Step 1	25° C for 10min
Step 2	42° C for 1 hour
Step 3	70° c for 10min

Before storage at -80° C, cDNA presence was checked by PCR with a housekeeping gene (*Gapdh*).

3.4.2. qRT-PCR

The qRT-PCR was kindly conducted in the laboratory of Prof. Dr. Frank Kolligs by Andrea Ofner.

For the qRT-PCR 96 well real-time PCR plates (Eppendorf, Hamburg), a heat sealing foil (Eppendorf, Hamburg), the intercalating fluorescent dye SYBR® Green (Lonza, Basel), the Taq DNA polymerase Kit and HotStar Taq polymerase (Quiagen, Hilden) were used. Total reaction volume was 20 µl. Reactions were run in a Mastercycler® ep realplex PCR machine (Eppendorf, Hamburg), with the following protocol:

Step 1:	95° C, 15 min (DNA denaturation)
Step 2:	95° C, 30 s (DNA denaturation)
Step 3:	55 °C, 30 s (primer annealing)
Step 4:	72° C, 30 s (elongation)
Step 5:	82° C, 20 s (DNA quantification)
Step 6:	95° C, 15 s (DNA denaturation)

- Step 7: 95° C, 15 s
- Step 8: continuously increasing heat to 95° C, 20 min (melting curve determination)
- Step 9: 95° C, 15 s

Steps 2 to 5 were repeated 55 times.

qRT-PCR data was analyzed with the deltaCT method as described (SCHMITTGEN & LIVAK, 2008).

IV. RESULTS

1. Results of transgenic mice generation

1.1. Confirmation of bone-specific overexpression of AREG and increased bone mass in Col1(I)-AREG mice

Bone specific overexpression of AREG in Col1(I)-AREG – transgenic mice was confirmed by Northern blot analysis for both L1 and L3 animals (unpublished data, not shown). The initial phenotypic characterization of this new mouse line also included the examination of the bones of transgenic animals and wild-type littermates by μ CT and peripheral quantitative computed tomography (pQCT) as described previously (SCHNEIDER et al., 2012).

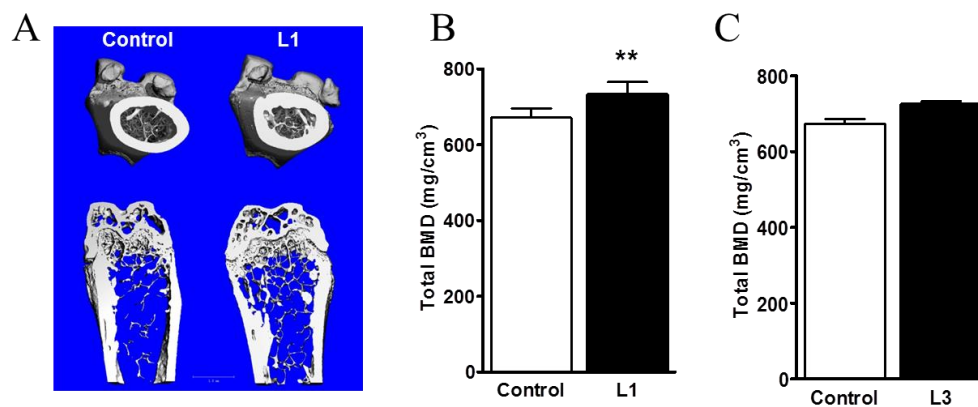


Figure 5: μ CT analysis of distal femur

Kindly provided by PD Dr. Marlon Schneider.

A: 3D image of distal femur of control and transgenic L1 mice; data for image obtained from μ CT analysis;

B: total bone mass density by μ CT analysis for L1 animals;

C: total bone mass density by μ CT analysis for L3 animals;

These measurements showed an increase in trabecular and total bone mineral density in the distal femur (μ CT) (**Figure 5**) and a significant increase in total bone mineral density in the distal femur (pQCT). The effect could be observed both in

L1 and L3 animals, so these results confirmed an AREG-induced anabolic effect on bones of the transgenic Col1(I)-AREG mouse-lines. Data shown in **Figure 5** were from 8 weeks old mice. Additionally, unpublished studies also revealed a decreased number of osteoclasts of Col1(I)-AREG mice (data not shown), which had been taken into special account for the analysis of the gene expression results. All the observed effects in Col1(I)-AREG mice were strongest in young age and completely disappeared with older age (unpublished data).

Figure 6 shows an example of a RT-PCR analysis for demonstrating expression of the transgene-derived *Areg*. As the primers for the Col1(I)-AREG transgenic mouse line are designed for the cDNA, there is no visible band in the wild-type mouse. Therefore, a loading control with a house keeping gene was necessary.

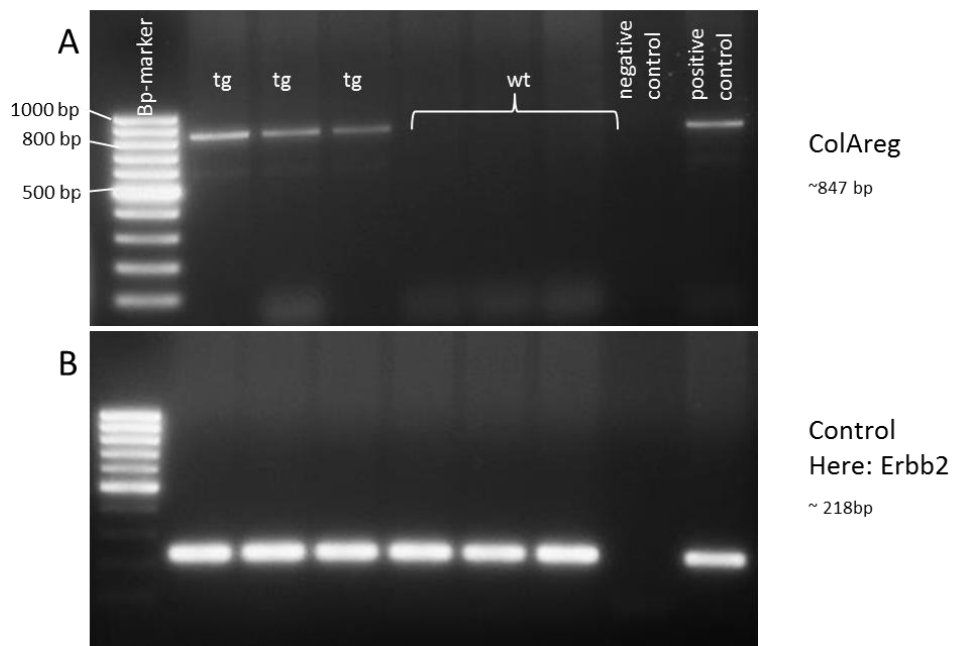


Figure 6: Example for PCR analysis

A: PCR analysis of Col1(I)-AREG transgenic and wild-type littermates; upstream primer located in exon 1, downstream primer located in exon 6 of the amphiregulin sequence, resulting in a 847 bp fragment for transgenic mice.

B: example for loading control (Erbb2); upstream and downstream primers both located in Intron 10 resulting in a 218 bp long fragment

for primer sequences see addendum IX.3.1

1.2. Killing of mice and bone collection

For the gene expression analysis, mice were killed at day 10 after birth for all animals of the 1 week group, at day 31 for the 4 weeks group and at day 57 after birth for the 8 weeks group. Mice were killed by cervical dislocation, or in the case of the 1 week group, beheaded by scissors. Both femurs were removed from the carcass, cleaned of remaining tissues with a paper towel, and immediately frozen on dry ice. There were no visible differences between the transgenic and the wild-type animals. The right femur of each animal was used for RNA isolation.

1.3. Body weight

All mice were weighed before necropsy. With the exception of the 8 weeks group, there were no significant differences in body weight between the transgenic and the wild-type animals (**Table 1**). In the 8 weeks group, wild-type animals were heavier than the transgenic mice.

Table 1: Weights of mice at the different ages.

Weights of wild-type and transgenic animals were compared by Student's t-test.

$p < 0.05$ was considered significant.

1 week group						4 weeks group					
Animal		Weight	Mean	SD	P-value	Animal		Weight	Mean	SD	P-value
84	tg	3.6				64	tg	17.53			
86	tg	4.33				73	tg	17.93			
87	tg	5.09				76	tg	17.18			
89	tg	5.67				77	tg	18.67			
97	tg	5.73	4.88	0.912		105	tg	18.29	17.92	0.591	
85	wt	5.09				63	wt	18.69			
88	wt	5.09				72	wt	18.72			
90	wt	5.24				74	wt	17.39			
95	wt	5.84				75	wt	14.28			
96	wt	6.15	5.48	0.484	0.232	108	wt	18.78	17.57	1.930	0.710
8 weeks group											
Animal		Weight	Mean	SD	P-value						
17	tg	20.02									
18	tg	21.42									
27	tg	18.85									
41	tg	20.11									
42	tg	20.50	20.18	0.927							
15	wt	21.54									
16	wt	20.54									
19	wt	21.19									
43	wt	22.90									
44	wt	21.86	21.61	0.874	0.037						

2. Microarray analysis

2.1. RNA quality analysis

RNA was isolated with Trizol Reagent (Life Technologies, Carlsbad) according to the manufacturer's instructions. The isolated RNA will be used to produce the labeled target, which, in turn, will be used to hybridize with the array. Therefore, RNA with a very high purity and integrity is essential to achieve reliable results.

To evaluate RNA quality and purity before processing to the microarray hybridization, Nanodrop measurement and gel electrophoresis were done.

The Nanodrop measurement yielded a ratio 260:280 in the range of 1.7 – 2.0 and a ratio 260:230 in the range of 2.1 – 2.5, indicating pure RNA, as contaminants like proteins, salts or others would be absorbing light at 230 nm or 280 nm.

Table 2: Results of Nanodrop measurement

SAMPLE ID	ng/ μ l	260/280	260/230
84_1week	161.82	1.96	2.46
86_1week	174.04	1.75	2.47
87_1week	211.99	1.76	2.47
90_1week_wt	176.06	1.72	2.48
95_1week_wt	233.48	1.76	2.47
96_1week_wt	306.87	1.78	2.4
64_4weeks	447.51	1.83	2.35
73_4weeks	579.46	2.01	2.21
77_4weeks	612.9	1.94	2.36
63_4weeks_wt	605.18	1.91	2.34
74_4weeks_wt	453.58	1.8	2.32
75_4weeks_wt	434.27	1.82	2.34
17_8weeks	412.82	1.8	2.38
18_8weeks	439.26	1.81	2.35
27_8weeks	380.71	1.82	2.37
15_8weeks_wt	598.98	1.86	2.13
16_8weeks_wt	462.63	1.83	2.36
19_8weeks_wt	447.58	1.85	2.29

Additionally, RNA integrity was analyzed, as purity does not indicate whether RNA is intact or not. To visualize intact RNA strands, a 1% agarose gel was prepared for gel electrophoresis. Two clear bands were visible, representing the 18S and 28S ribosomal RNA, indicating intact RNA (**Figure 7**). A ratio 28S:18S of 2 is typical

for intact RNA. An analysis on agarose gel was done additionally for quality control to exclude a possible contamination with genomic DNA which would not have been detected by the Bioanalyzer. The area of possible contamination with genomic DNA is marked on the image section (**Figure 7**).

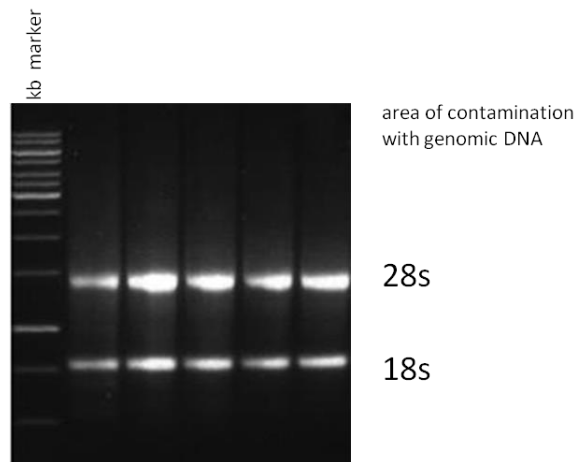


Figure 7: RNA quality analysis on agarose gel

Integrity of RNA used for the microarray was furthermore confirmed with the Bioanalyzer (Agilent 2100 Bioanalyzer, Agilent, Waldbronn), a microfluidic instrument, that is more sensitive and able to analyze smaller amounts of RNA. Data can be visualized as a gel-like image or an electrospherogram. **Figure 8** shows the gel-like image of the analysis with the Bioanalyzer.

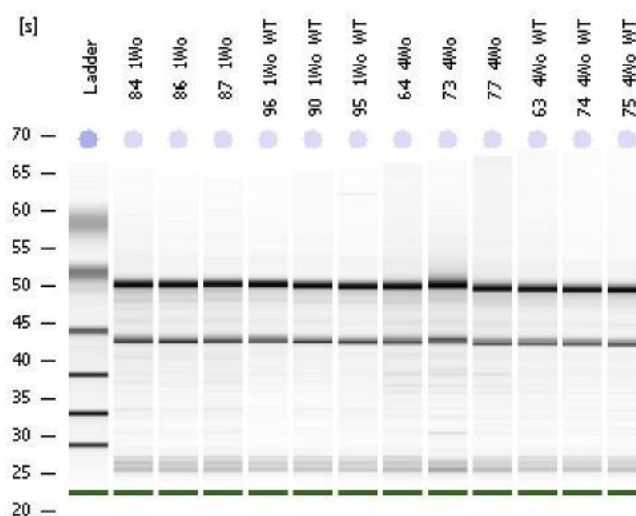


Figure 8: Gel-like image of RNA-analysis with Bioanalyzer

The Bioanalyzer evaluates RNA integrity by RIN (RNA integrity number), a standardized tool for RNA quality assessment. A RIN of 1 stands for the highest degradation grade, 10 for best quality. All samples ranked from RIN 8.5 – 10 (**Figure 9**).

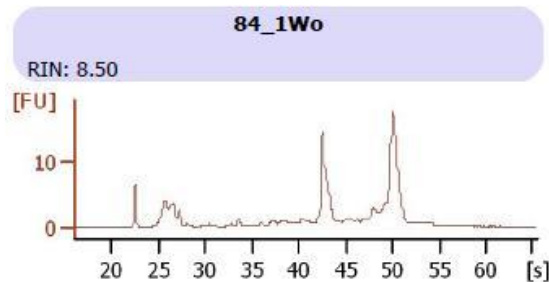


Figure 9: Example for RIN-quality analysis with the Bioanalyzer

2.2. Statistical and bioinformatical analysis of the array data

After hybridization, the slides were scanned with an Agilent DNA Microarray Scanner (G2505C, Agilent, Waldbronn), and image processing was performed with Feature Extraction Software 10.5.1.1. (Agilent, Waldbronn). Probes were first filtered for those which are above background noise before data normalization with VSN, version 3.18.0 (HUBER et al., 2002). Quality control of the normalized data was conducted with an Euclidian distance matrix. The output data is a heat map, which shows high similarity of the data coded in red or otherwise lowest similarity coded in dark blue.

Figure 10 shows the resulting heat maps of this quality control. Additionally to the color code, the branches of the cluster trees indicate the clustering of genes. For the 1 week and the 4 weeks groups (**Figure 10**, A and B), wild-types were clustering together, as were the transgenic animals. For the 8 weeks group, two animals had to be excluded, because of aberration. But the branches of the cluster tree indicate that, nevertheless, no satisfactory clustering for each wild-types and transgenics could be achieved (**Figure 10**, C).

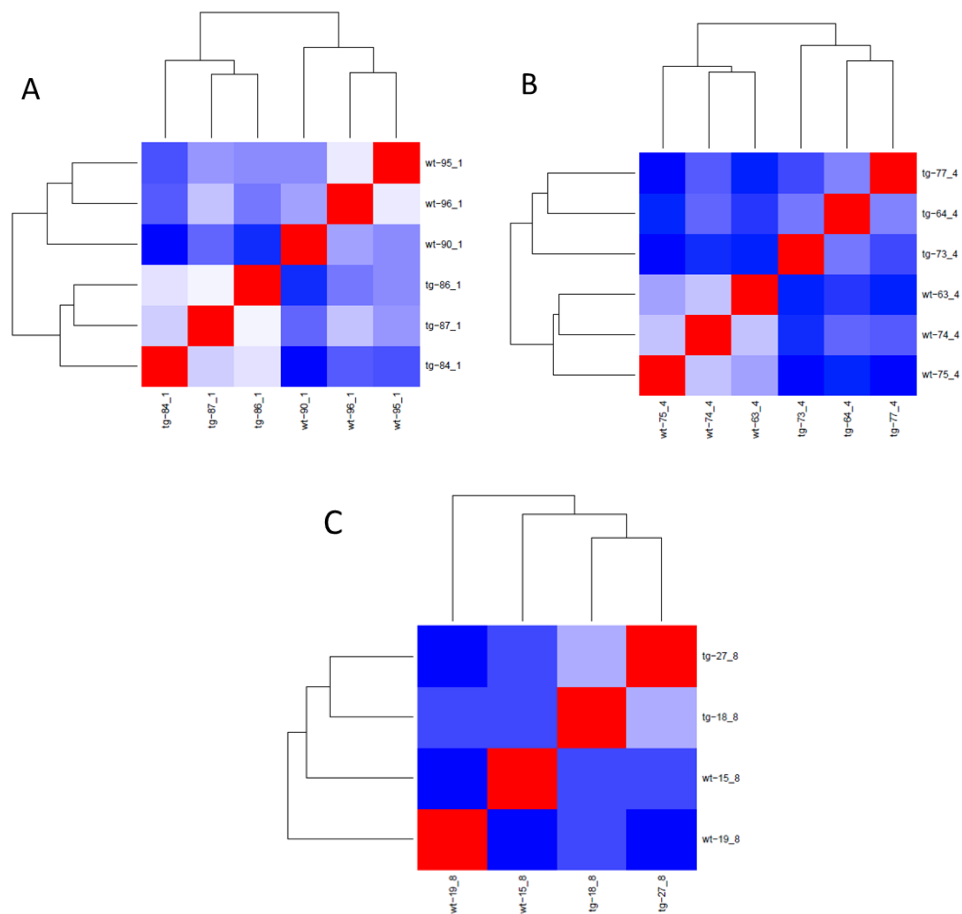


Figure 10: Heatmaps

A: Heatmap of 1 week group

B: Heatmap of 4 weeks group

C: Heatmap of 8 weeks group

Significance analysis to detect differentially expressed genes was done with Limma, version 3.6.9. Genes with a two-fold difference in expression (Log_2 Fold change ≥ 1 for upregulated genes; Log_2 Fold change ≤ -1 for downregulated genes) with an adjusted p-value < 0.05 were considered significant. To further analyze the obtained genes, a SOTA (self-organizing-tree-algorithm) - analysis was conducted. The principle behind this analysis is to cluster differentially expressed genes with a similar expression pattern (HERRERO et al., 2001). For each age-group, two clusters of genes were grouped (**Figure 11**). The highest amount of clustering genes could be detected in the 1 week group (184 down-regulated genes, 47 up-regulated genes), with a distinct drop in the number of clustering genes in the 4 weeks group (8 down-regulated genes, 56 up-regulated genes) and no differentially expressed

genes clustering together in the 8 weeks group.

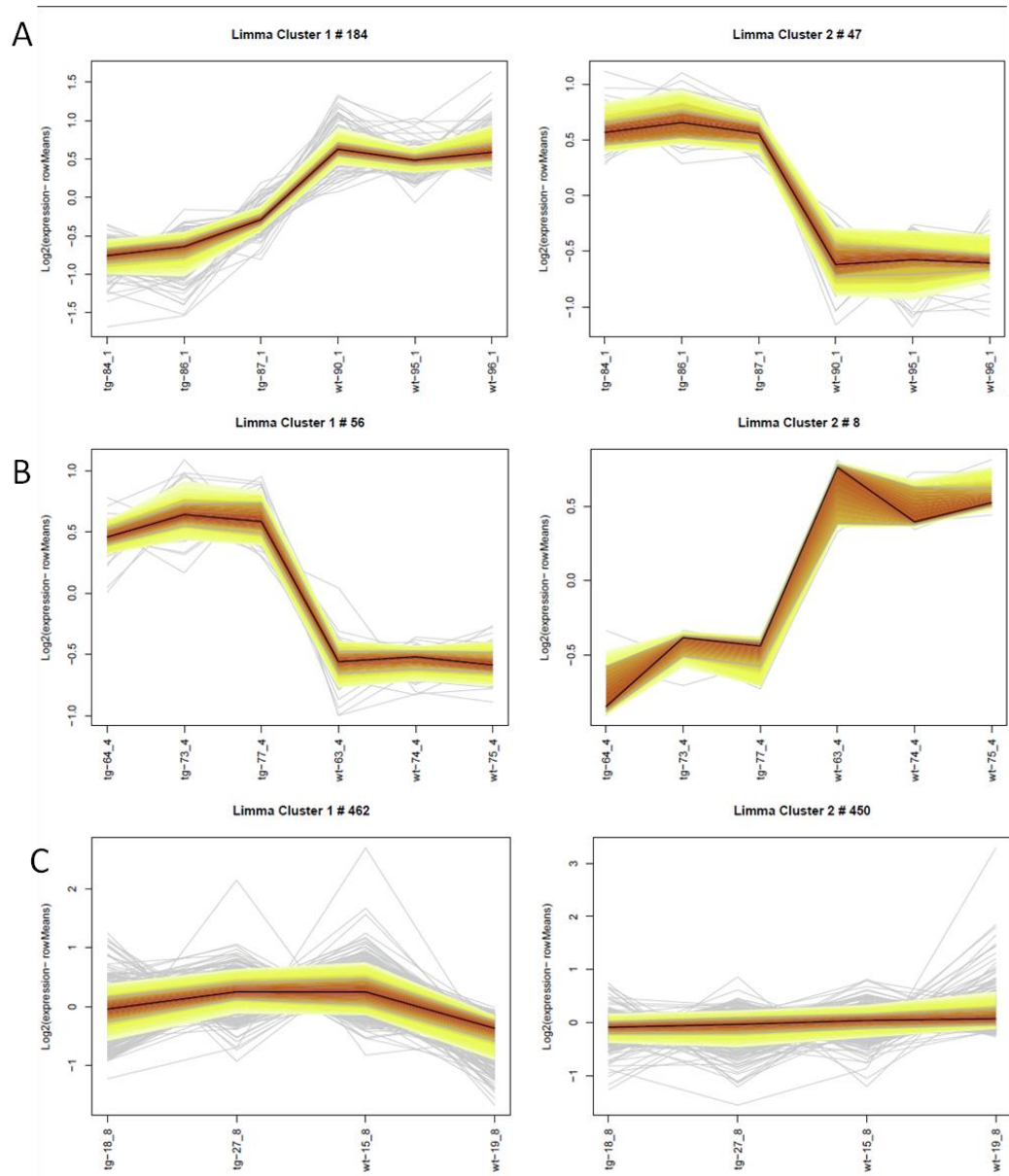


Figure 11: Sota-cluster analysis

A: Cluster-analysis for 1 week age-group; 184 down-regulated (left) and 47 up-regulated (right) genes for transgenic animals compared to wild-type control

B: Cluster-analysis for 4 weeks age-group; 56 up-regulated (left) and 8 down-regulated (right) genes for transgenic animals compared to wild-type control

C: Cluster-analysis for 8 weeks age-group; 462 and 450 genes clustering; no distinct up- or down-regulation

Figure 11 shows that the number of differentially regulated genes that could be found decreased with age. In the 8 weeks group the array results showed no difference between the transgenic compared to the wild-type group. So the most significant effect was observed in the youngest group. This effect might be indicating that other genes are possibly compensating the effect of bone-specific AREG overexpression.

2.2.1. GO Analysis

Transcriptome analyses yield results up to thousands of genes, which makes it impossible to analyze the dataset gene by gene. Appropriate tools have been developed to enable not only the analysis of single genes but a functional annotation of huge datasets. They are based on the standardized “gene vocabulary” developed by the Gene Ontology Consortium (ASHBURNER et al., 2000) comprising the three categories biological process, molecular function and cellular component. A given set of genes can be analyzed with these tools to search for enriched terms, to get a general idea of the connection of those genes.

For this work, a tool provided by the free online bioinformatics resource DAVID (Database for Annotation, Visualization, and Integrated Discovery) (Version: 6.7) (DENNIS et al., 2003) was used to search for enriched GO-terms in the categories mentioned above: the Functional Annotation Clustering Tool. This tool is able to measure the “relationship” of annotated terms from different sources and groups them together in annotation groups, thus reducing redundant terms and enabling to visualize directly overrepresented categories without searching through long lists of annotation terms. Additionally, the open source bioinformatics network Cytoscape (Version: 3.0.2) was used. Cytoscape (SHANNON et al., 2003) was used with the plug-ins CluGo (Version: 2.0.7) (BINDEA et al., 2009) and CluPedia (Version: 1.0.8) (BINDEA et al., 2013) to create a network graph, with nodes and edges as links, thus visualizing correlation between the found terms and the genes selected by Cytoscape for the enriched terms. CluGo integrates not only GoTerms (ASHBURNER et al., 2000), but also KEGG/BioCarta pathways (KANEHISA, 2002) to create a functionally organized GO/pathway term network; it enables to analyze a single list of genes or to compare different lists of genes and to visualize their functional differences/relationships in a color coded network graph (BINDEA et al., 2009).

2.2.2. Differentially expressed genes of the 1 week group

The lists of differentially expressed genes for this group can be found in IX.4.1 and IX.4.2. 47 up-regulated and 184 down-regulated differentially expressed genes could be found for the 1 week group.

Functional annotation clustering analysis of the obtained lists of differentially expressed genes was conducted using the free web-based database DAVID.

Table 3: DAVID – selected Functional Annotation Cluster-results for 1 week group, up-regulated genes

(Numbers in brackets are number of genes and fold enrichment of the functional term;

Enrichment score is geometric mean of member's p-values of corresponding annotation cluster (in $-\log$ scale))

Representative functional terms of overrepresented annotation clusters	Enrichment score
Extracellular region (13, 4.2), secreted (10, 4.1), disulfide bond (12, 2.8), signal peptide (13, 2.2)	3.1
Egf-like domain (4, 10.4)	2.1
Neuron differentiation (5, 6.1), neuron development (4, 6.6)	1.4
Regulation of apoptosis (5, 4.9) positive regulation of apoptosis (3, 5.9)	1.3

The analysis of the differentially expressed up-regulated genes yielded GO-terms for biological processes in the extracellular region, EGF-like domain, nervous system development and apoptosis (see **Table 3**). **Table 4** lists the genes sorted by DAVID to the annotation terms of **Table 3**.

Table 4: Gene List to Annotation terms for 1 week group, up-regulated genes

Annotation Term	Genes
Extracellular region	Spp1, Msln, S100b, Col25a1, Slit2, Timp1, EMI, Plat, Gcg, SrpX2, Enpp1, Fbn2, Mmp9
Secreted	Spp1, Msln, Slit2, Timp1, EMI, Plat, Gcg, SrpX2, Fbn2, Mmp9
Disulfide bond	Unc-5b, Slit2, Timp1, EMI, Plat, SrpX2, Enpp1, Fbn2, Mmp9, Megf10, Gzme, Klrb1a
Signal peptide	Spp1, Msln, Unc-5b, Slit2, Timp1, EMI, Plat, Gcg, SrpX2, Fbn2, Mmp9, Gzme, Megf10
EGF-like domain	Megf10, Slit2, Fbn2, Plat
Neuron differentiation	Dlx2, Uchl1, Etv4, Map1b, Slit2
Neuron development	Uchl1, Etv4, Map1b, Slit2
Regulation of apoptosis	Spp1, S100b, Cdkn2a, Timp1, Mmp9
Positive regulation of apoptosis	S100b, Cdkn2a, Mmp9

The analysis of the up-regulated genes with the program Cytoscape yielded results in the form of a diagram visualizing the connections between the genes and the biological processes as nodes and edges (**Figure 12**), the same analysis also being presented as table (see **Table 5**). **Figure 12** and **Table 5** show clearly that there are 2 genes, *Dcstamp* and *Spp1*, overrepresented in biological processes regarding bone metabolism.

Spp1 (also known as Osteopontin, OPN) is one of the genes overrepresented in both analyses. DAVID and Cytoscape also revealed genes like for example *Enpp1*, *Slit2*, *Map1b* (or also known as Mtap1b) and *Cdkn2a* (also known as p16) in annotation terms regarding growth in general.

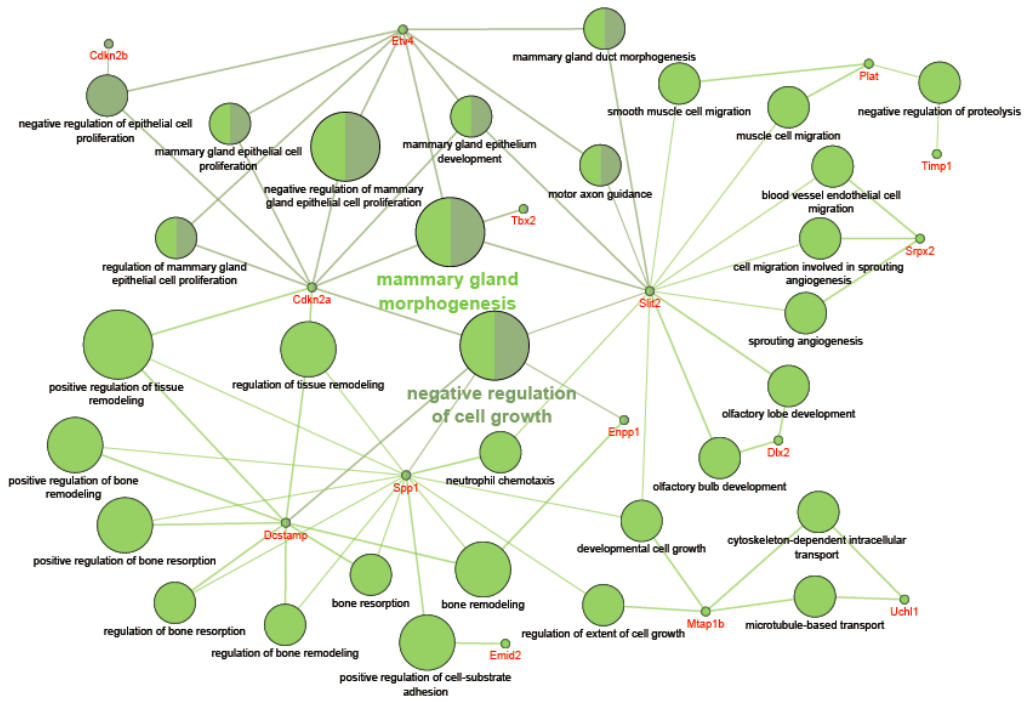


Figure 12: Cytoscape diagram of 1 week group, up-regulated genes

Table 5: Genes corresponding to biological processes for 1 week group, up-regulated genes

NAME	Cdkn2a	Cdkn2b	Dcstamp	Dlx2	Emid2	Enpp1	Etv4	Mtap1b	Plat	Sirt2	Spp1	Srxp2	Tbx2	Timp1	Uchl1
sprouting angiogenesis	0	0	0	0	0	0	0	0	0	1	0	1	0	0	0
cell migration involved in sprouting angiogenesis	0	0	0	0	0	0	0	0	0	1	0	1	0	0	0
motor axon guidance	0	0	0	0	0	0	1	0	0	1	0	0	0	0	0
positive regulation of cell-substrate adhesion	0	0	0	0	1	0	0	0	0	0	1	0	0	0	0
microtubule-based transport	0	0	0	0	0	0	0	1	0	0	0	0	0	0	1
muscle cell migration	0	0	0	0	0	0	0	0	1	1	0	0	0	0	0
smooth muscle cell migration	0	0	0	0	0	0	0	0	1	1	0	0	0	0	0
olfactory bulb development	0	0	0	1	0	0	0	0	0	1	0	0	0	0	0
olfactory lobe development	0	0	0	1	0	0	0	0	0	1	0	0	0	0	0
negative regulation of cell growth	1	0	1	0	0	1	0	0	0	1	1	0	0	0	0
neutrophil chemotaxis	0	0	0	0	0	0	0	0	0	1	1	0	0	0	0
cytoskeleton-dependent intracellular transport	0	0	0	0	0	0	0	1	0	0	0	0	0	0	1
mammary gland epithelial cell proliferation	1	0	0	0	0	0	1	0	0	0	0	0	0	0	0
regulation of mammary gland epithelial cell proliferation	1	0	0	0	0	0	1	0	0	0	0	0	0	0	0
negative regulation of mammary gland epithelial cell proliferation	1	0	0	0	0	0	1	0	0	0	0	0	0	0	0
regulation of tissue remodeling	1	0	1	0	0	0	0	0	0	0	1	0	0	0	0
positive regulation of tissue remodeling	1	0	1	0	0	0	0	0	0	0	1	0	0	0	0
blood vessel endothelial cell migration	0	0	0	0	0	0	0	0	0	1	0	1	0	0	0
regulation of bone resorption	0	0	1	0	0	0	0	0	0	0	1	0	0	0	0
bone resorption	0	0	1	0	0	0	0	0	0	0	1	0	0	0	0
positive regulation of bone resorption	0	0	1	0	0	0	0	0	0	0	1	0	0	0	0
bone remodeling	0	0	1	0	0	1	0	0	0	0	1	0	0	0	0
regulation of bone remodeling	0	0	1	0	0	0	0	0	0	0	1	0	0	0	0
positive regulation of bone remodeling	0	0	1	0	0	0	0	0	0	0	1	0	0	0	0
developmental cell growth	0	0	0	0	0	0	0	1	0	1	1	0	0	0	0
negative regulation of epithelial cell proliferation	1	1	0	0	0	0	1	0	0	0	0	0	0	0	0
mammary gland morphogenesis	1	0	0	0	0	0	1	0	0	1	0	0	1	0	0
mammary gland duct morphogenesis	0	0	0	0	0	0	1	0	0	1	0	0	0	0	0
mammary gland epithelium development	1	0	0	0	0	0	1	0	0	1	0	0	0	0	0
regulation of extent of cell growth	0	0	0	0	0	0	0	1	0	0	1	0	0	0	0
negative regulation of proteolysis	0	0	0	0	0	0	0	0	1	0	0	0	0	1	0

For the differentially expressed down-regulated genes, DAVID found GO-terms in the categories hematopoiesis and immune system development, amino acid transport and cytoskeleton organization (**Table 6**). The differentially expressed genes belonging to the annotation terms of **Table 6** are listed in **Table 7**.

Table 6: DAVID – selected Functional Annotation Cluster-results for 1 week group, down-regulated genes

(Numbers in brackets are number of genes and fold enrichment of the functional term;

Enrichment score is geometric mean of member's P values of corresponding annotation cluster (in $-\log$ scale))

Representative functional terms of overrepresented annotation clusters	Enrichment score
Porphyrin biosynthetic process (5, 53.9), cofactor biosynthetic process (7, 14.9), heme biosynthesis (4, 52.8)	4.5
Erythrocyte differentiation (6, 24.3), myeloid cell differentiation (7, 14.2), immune system development (8, 5.3)	3.2
Amino acid transport (4, 10.9)	1.7
Cytoskeleton organization (7, 3.0)	1.6

Table 7: Gene List to Annotation terms for 1 week group, down-regulated genes

Annotation Term	Genes
Porphyrin biosynthetic process	Alas2, Spta1, Uros, hydroxymethylbilane synthase, Fech
Cofactor biosynthetic process	Nmnat3, Alas2, Gch1, Spta1, Fech, hydroxymethylbilane synthase, Uros
Heme biosynthesis	Alas2, Fech, Uros, hydroxymethylbilane synthase
Erythrocyte differentiation	Alas2, Tal1, Trim10, Klf1, Fech, Epb4.2
Myeloid cell differentiation	Alas2, Spib, Tal1, Trim10, Klf1, Fech, Epb4.2
Immune system development	Alas2, Spib, Tal1, Trim10, Klf1, Fech, Spta1, Epb4.2
Amino acid transport	Slc6a20, Slc22a4, Slc6a9, Slc43a1
Cytoskeletal protein binding	Fhdc1, Kif18a, Epb4.2, Aqp2, Spta1, Slc4a1, Tensin4

The differentially down-regulated genes were also analyzed with Cytoscape. For the diagram see **Figure 13**.

Table 8 shows the genes from the diagram attributed to the biological processes. The Cytoscape analysis yielded results similar to those obtained with DAVID (**Table 7**); overrepresented terms were biological processes associated with hematopoiesis, genes found by both programs for several annotation terms were for example *Alas2*, *Fech*, *Tal1*. Genes associated with bone metabolism were not detected.

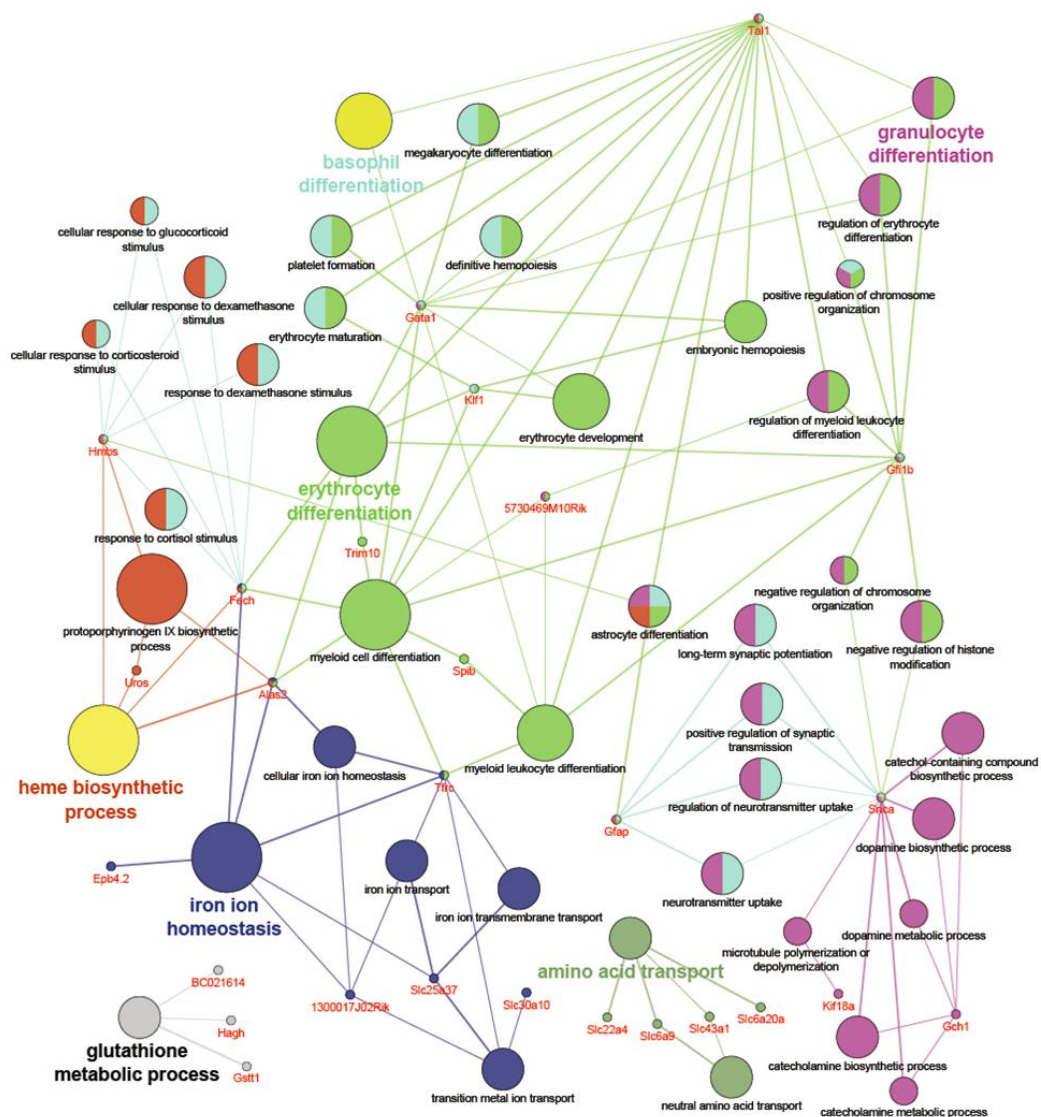


Figure 13: Cytoscape diagram of 1 week group, down-regulated genes

Table 8: Genes corresponding to biological processes for 1 week group, down-regulated genes

NAME	1300017J02Rik	5730469M10Rik	Alas2	BCO21614	Epb4.2	Fech	Gata1	Gch1	Gfap	Gfl1b	Gstt1	Hagh	Hmbs	Klf18a	Klf1	Slc22a4	Slc25a37	Slc30a10	Slc43a1	Slc6a20a	Slc6a9	Sncg	Spib	Tal1	Tfrc	Trm10	Uros
transition metal ion transport	1	0	0	0	0	0	0	0	0	0	0	0	0	0	0	0	0	0	0	0	0	0	0	0	0	0	0
neurotransmitter uptake	0	0	0	0	0	0	0	0	1	0	0	0	0	0	0	0	0	0	0	0	0	0	1	0	0	0	0
myeloid leukocyte differentiation	0	1	0	0	0	0	1	0	0	1	0	0	0	0	0	0	0	0	0	0	0	0	0	1	1	1	0
regulation of myeloid leukocyte differentiation	0	1	0	0	0	0	0	0	0	1	0	0	0	0	0	0	0	0	0	0	0	0	0	0	0	1	0
catecholamine metabolic process	0	0	0	0	0	0	0	1	0	0	0	0	0	0	0	0	0	0	0	0	0	0	1	0	0	0	0
glutathione metabolic process	0	0	1	0	0	0	0	0	0	1	1	0	0	0	0	0	0	0	0	0	0	0	0	0	0	0	0
protoporphyrinogen IX biosynthetic process	0	0	1	0	0	0	0	0	0	0	0	0	1	0	0	0	0	0	0	0	0	0	0	0	0	0	1
heme biosynthetic process	0	0	1	0	0	1	0	0	0	0	0	0	1	0	0	0	0	0	0	0	0	0	0	0	0	0	1
iron ion transport	1	0	0	0	0	0	0	0	0	0	0	0	0	0	0	1	0	0	0	0	0	0	0	0	1	0	0
amino acid transport	0	0	0	0	0	0	0	0	0	0	0	0	0	0	0	1	0	0	1	1	1	0	0	0	0	0	0
cellular iron ion homeostasis	1	0	1	0	0	0	0	0	0	0	0	0	0	0	0	0	0	0	0	0	0	0	0	0	1	0	0
catechol-containing compound biosynthetic process	0	0	0	0	0	0	1	0	0	0	0	0	0	0	0	0	0	0	0	0	0	1	0	0	0	0	0
neutral amino acid transport	0	0	0	0	0	0	0	0	0	0	0	0	0	0	0	0	0	0	1	0	1	0	0	0	0	0	0
myeloid cell differentiation	0	1	1	0	0	1	1	0	0	1	0	0	0	0	1	0	0	0	0	0	0	0	1	1	1	1	0
erythrocyte differentiation	0	0	1	0	0	1	1	0	0	1	0	0	0	0	1	0	0	0	0	0	0	0	0	0	1	0	1
megakaryocyte differentiation	0	0	0	0	0	0	1	0	0	0	0	0	0	0	0	0	0	0	0	0	0	0	0	1	0	0	0
platelet formation	0	0	0	0	0	0	1	0	0	0	0	0	0	0	0	0	0	0	0	0	0	0	0	1	0	0	0
basophil differentiation	0	0	0	0	0	0	1	0	0	0	0	0	0	0	0	0	0	0	0	0	0	0	0	0	1	0	0
granulocyte differentiation	0	0	0	0	0	1	0	0	1	0	0	0	0	0	0	0	0	0	0	0	0	0	0	0	1	0	0
negative regulation of histone modification	0	0	0	0	0	0	0	0	1	0	0	0	0	0	0	0	0	0	0	0	0	1	0	0	0	0	0
microtubule polymerization or depolymerization	0	0	0	0	0	0	0	0	0	0	0	0	0	1	0	0	0	0	0	0	0	1	0	0	0	0	0
iron ion transmembrane transport	0	0	0	0	0	0	0	0	0	0	0	0	0	0	0	1	0	0	0	0	0	0	0	0	1	0	0
embryonic hemopoiesis	0	0	0	0	0	1	0	0	0	0	0	0	0	0	0	1	0	0	0	0	0	0	0	0	1	0	0
dopamine biosynthetic process	0	0	0	0	0	0	0	1	0	0	0	0	0	0	0	0	0	0	0	0	0	0	1	0	0	0	0
dopamine metabolic process	0	0	0	0	0	0	1	0	0	0	0	0	0	0	0	0	0	0	0	0	0	1	0	0	0	0	0
catecholamine biosynthetic process	0	0	0	0	0	0	1	0	0	0	0	0	0	0	0	0	0	0	0	0	0	0	1	0	0	0	0
erythrocyte maturation	0	0	0	0	0	0	0	0	0	0	0	0	0	0	0	1	0	0	0	0	0	0	0	0	1	0	0
regulation of erythrocyte differentiation	0	0	0	0	0	1	0	0	1	0	0	0	0	0	0	0	0	0	0	0	0	0	0	0	1	0	0
astrocyte differentiation	0	0	0	0	0	0	0	1	0	0	0	1	0	0	0	0	0	0	0	0	0	0	0	0	1	0	0
erythrocyte development	0	0	0	0	0	1	0	0	0	0	0	0	0	0	0	1	0	0	0	0	0	0	0	0	1	0	0
positive regulation of synaptic transmission	0	0	0	0	0	0	0	1	0	0	0	0	0	0	0	0	0	0	0	0	0	1	0	0	0	0	0
response to cortisol stimulus	0	0	0	0	0	1	0	0	0	0	0	0	1	0	0	0	0	0	0	0	0	0	0	0	0	0	0
regulation of neurotransmitter uptake	0	0	0	0	0	0	0	0	1	0	0	0	0	0	0	0	0	0	0	0	0	1	0	0	0	0	0
iron ion homeostasis	1	0	1	0	1	1	0	0	0	0	0	0	0	0	0	0	1	0	0	0	0	0	0	0	0	1	0
definitive hemopoiesis	0	0	0	0	0	0	1	0	0	0	0	0	0	0	0	0	0	0	0	0	0	0	0	0	1	0	0
long-term synaptic potentiation	0	0	0	0	0	0	0	1	0	0	0	0	0	0	0	0	0	0	0	0	0	1	0	0	0	0	0
cellular response to corticosteroid stimulus	0	0	0	0	0	1	0	0	0	0	0	0	0	0	0	0	0	0	0	0	0	0	0	0	0	0	0
cellular response to glucocorticoid stimulus	0	0	0	0	0	1	0	0	0	0	0	0	1	0	0	0	0	0	0	0	0	0	0	0	0	0	0
response to dexamethasone stimulus	0	0	0	0	0	1	0	0	0	0	0	0	1	0	0	0	0	0	0	0	0	0	0	0	0	0	0
cellular response to dexamethasone stimulus	0	0	0	0	0	1	0	0	0	0	0	0	1	0	0	0	0	0	0	0	0	0	0	0	0	0	0
negative regulation of chromosome organization	0	0	0	0	0	0	0	0	0	1	0	0	0	0	0	0	0	0	0	0	0	1	0	0	0	0	0
positive regulation of chromosome organization	0	0	0	0	0	0	0	0	0	1	0	0	0	0	0	0	0	0	0	0	0	0	0	1	0	0	0

2.2.3. Differentially expressed genes of the 4 weeks group

56 differentially up-regulated genes and 8 down-regulated genes could be identified for this group (IX.4.3 and IX.4.4).

DAVID yielded a functional annotation clustering report only for the up-regulated genes (**Table 9**). Found GO-terms were mainly extracellular region and embryonic limb morphogenesis.

Table 9: DAVID – selected Functional Annotation Cluster-results for 4 weeks group, up-regulated genes

(Numbers in brackets are number of genes and fold enrichment of the functional term;

Enrichment score is geometric mean of member's P values of corresponding annotation cluster (in $-\log$ scale))

Representative functional terms of overrepresented annotation clusters	Enrichment score
Extracellular region part (16, 3.9)	5.4
Cell adhesion (10, 8.4)	4.5
egf-like domain (6, 13.8), metal ion binding (7, 0.9)	2.6
Embryonic limb morphogenesis (3, 14.5)	1.5
Neuron development (4, 6.4)	1.3

Table 10: Gene List to Annotation terms for 4 weeks group, up-regulated genes

Annotation Term	Genes
Extracellular region	Spp1, Ecm1, Msln, Col25a1, Timp1, Slit2, Col8a1, Col5a3, Plat, Epha3, Tnc, Lama2, Srp2, Fbln1, Enpp1, Fbn2
Cell adhesion	Spp1, Tnc, Megf10, Lama2, Msln, Cdh11, Col8a1, Pcdhga, Gpnmb, Col5a3
Egf-like domain	Tnc, Megf10, Slit2, Fbln1, Fbn2, Plat
Metal ion binding	Cyp2s1, Cdh11, Slit2, Fbln1, Enpp1, Pcdhga, Fbn2
Embryonic limb morphogenesis	Prrx2, Prrx1, Fbn2
Neuron development	Uchl1, Slitrk6, Map1b, Slit2

The Cytoscape analysis yielded similar results, with terms for biological processes regarding growth, proliferation and differentiation of cells in general. Overrepresented genes found by both programs were again *Spp1* and *Slit2*, along with *Prrx1* and *Prrx2* (**Figure 14** and **Table 11**).

The small number of the down-regulated genes did not yield any annotation results by both DAVID and Cytoscape.

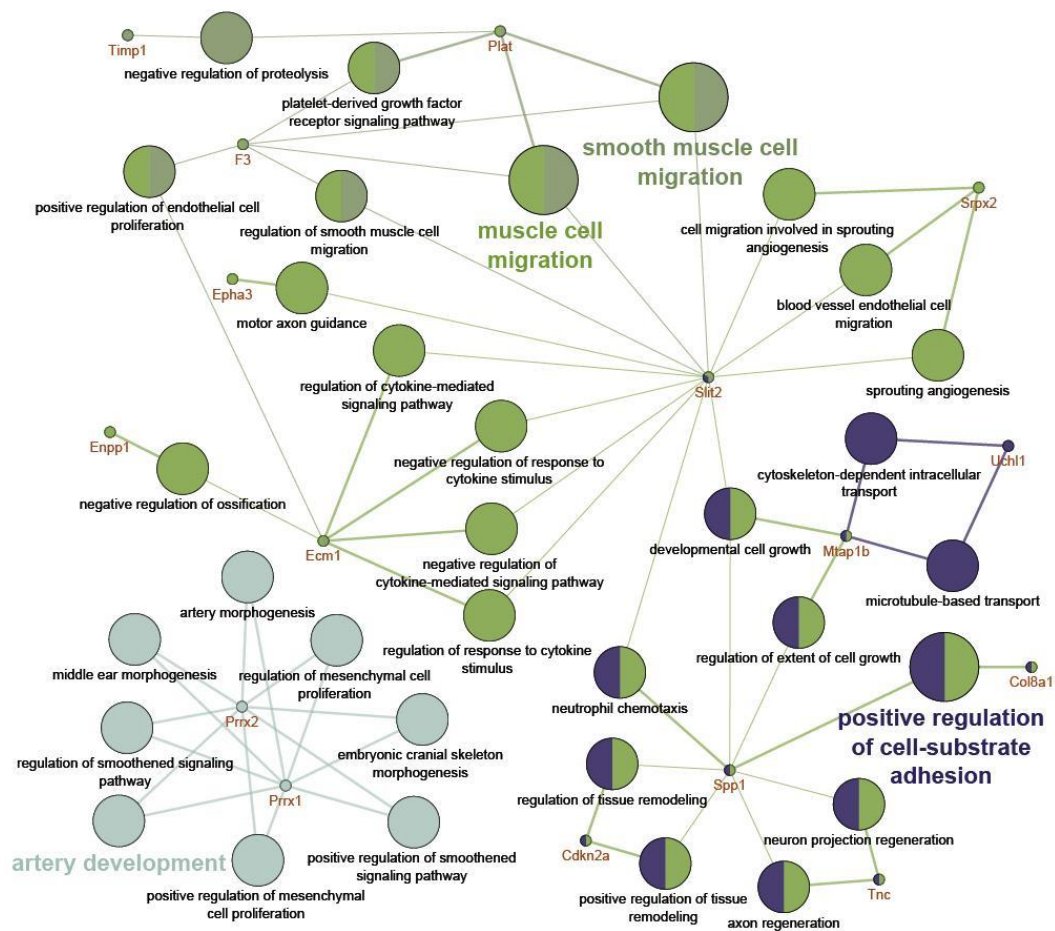


Figure 14: Cytoscape diagram of 4 weeks group, up-regulated genes

Table 11: Genes corresponding to biological processes for 4 weeks group, up-regulated genes

NAME	Cdkn2a	Col8a1	Ecm1	Enpp1	Epha3	F3	Mtap1b	Plat	Prrx1	Prrx2	Slt2	Spp1	Srpx2	Timp1	Tnc	Uchl1
positive regulation of endothelial cell proliferation	0	0	1	0	0	1	0	0	0	0	0	0	0	0	0	0
regulation of cytokine-mediated signaling pathway	0	0	1	0	0	0	0	0	0	0	1	0	0	0	0	0
negative regulation of cytokine-mediated signaling pathway	0	0	1	0	0	0	0	0	0	0	1	0	0	0	0	0
sprouting angiogenesis	0	0	0	0	0	0	0	0	0	0	1	0	1	0	0	0
cell migration involved in sprouting angiogenesis	0	0	0	0	0	0	0	0	0	0	1	0	1	0	0	0
positive regulation of mesenchymal cell proliferation	0	0	0	0	0	0	0	0	1	1	0	0	0	0	0	0
motor axon guidance	0	0	0	0	1	0	0	0	0	0	1	0	0	0	0	0
regulation of smoothened signaling pathway	0	0	0	0	0	0	0	0	1	1	0	0	0	0	0	0
regulation of mesenchymal cell proliferation	0	0	0	0	0	0	0	0	1	1	0	0	0	0	0	0
positive regulation of cell-substrate adhesion	0	1	0	0	0	0	0	0	0	0	0	1	0	0	0	0
microtubule-based transport	0	0	0	0	0	0	1	0	0	0	0	0	0	0	0	1
muscle cell migration	0	0	0	0	0	1	0	1	0	0	1	0	0	0	0	0
smooth muscle cell migration	0	0	0	0	0	1	0	1	0	0	1	0	0	0	0	0
regulation of smooth muscle cell migration	0	0	0	0	1	0	0	0	0	1	0	0	0	0	0	0
negative regulation of ossification	0	0	1	1	0	0	0	0	0	0	0	0	0	0	0	0
neutrophil chemotaxis	0	0	0	0	0	0	0	0	0	0	1	1	0	0	0	0
cytoskeleton-dependent intracellular transport	0	0	0	0	0	0	1	0	0	0	0	0	0	0	0	1
neuron projection regeneration	0	0	0	0	0	0	0	0	0	0	0	1	0	0	1	0
axon regeneration	0	0	0	0	0	0	0	0	0	0	0	1	0	0	1	0
regulation of tissue remodeling	1	0	0	0	0	0	0	0	0	0	0	1	0	0	0	0
positive regulation of tissue remodeling	1	0	0	0	0	0	0	0	0	0	0	1	0	0	0	0
middle ear morphogenesis	0	0	0	0	0	0	0	0	1	1	0	0	0	0	0	0
blood vessel endothelial cell migration	0	0	0	0	0	0	0	0	0	0	1	0	1	0	0	0
negative regulation of proteolysis	0	0	0	0	0	0	0	1	0	0	0	0	0	1	0	0
positive regulation of smoothened signaling pathway	0	0	0	0	0	0	0	0	1	1	0	0	0	0	0	0
platelet-derived growth factor receptor signaling pathway	0	0	0	0	0	1	0	1	0	0	0	0	0	0	0	0
developmental cell growth	0	0	0	0	0	0	1	0	0	0	1	1	0	0	0	0
embryonic cranial skeleton morphogenesis	0	0	0	0	0	0	0	0	1	1	0	0	0	0	0	0
artery morphogenesis	0	0	0	0	0	0	0	0	1	1	0	0	0	0	0	0
regulation of response to cytokine stimulus	0	0	1	0	0	0	0	0	0	0	1	0	0	0	0	0
negative regulation of response to cytokine stimulus	0	0	1	0	0	0	0	0	0	0	1	0	0	0	0	0
artery development	0	0	0	0	0	0	0	0	1	1	0	0	0	0	0	0
regulation of extent of cell growth	0	0	0	0	0	0	1	0	0	0	0	1	0	0	0	0

2.2.4. Differentially expressed genes of the 8 weeks group

In this age-group, no differentially expressed genes were revealed by the microarray analysis, except for *Areg*, which could still be detected by microarray with a 24.2-fold up-regulation.

2.3. qRT-PCR results

qRT-PCR was conducted to verify a small selection of genes (*Dcstamp* and *Mmp9*) identified by the microarray analysis and to examine two other genes known to influence osteoclast differentiation (*Rankl* and *Opg*) which had not been detected by microarray analysis. *Gapdh* was employed as a house keeping gene. The qRT-PCR was only done for the 1 week group. The sequences of the primers can be found in IX.3.2.

As **Figure 15** shows, the results differ from the ones of the microarray analysis. None of the examined genes was significantly regulated. While the analysis via

microarray indicated that the levels of *Mmp9* and *Dcstamp* of the transgenic animals were increased compared to the wild-type control, the qRT-PCR analysis did not confirm this result. For *Rankl* and *Opg*, which had not been detected by microarray analysis, no significant up- or down-regulation was detected by qRT-PCR either.

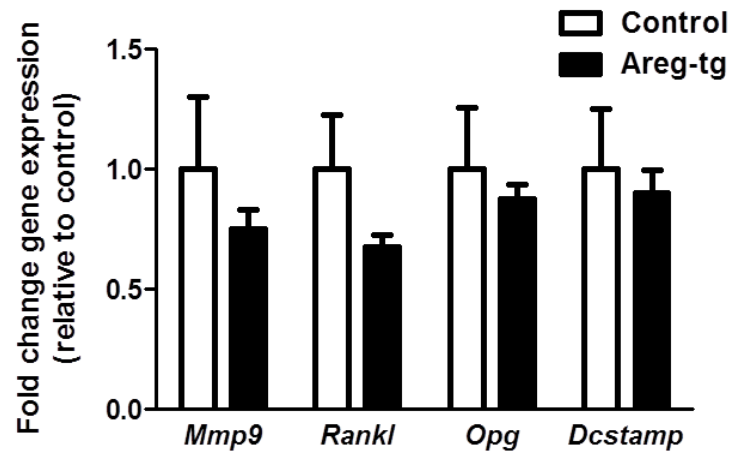


Figure 15: Results of qRT-PCR

V. DISCUSSION

Amphiregulin has been identified as a possible PTH-target gene, and might be one of the factors influencing the anabolic actions of PTH on bone formation via the EGFR. The aim of this work was to search for genes up- or down-regulated in the bones of transgenic mice overexpressing *Areg*, which show an increase in bone mass.

1.1. Col1(I)-AREG mouse line for transcriptome analysis

A transgenic mouse line, the Col1(I)-AREG mouse line, had been generated to obtain osteoblast-specific *Areg* overexpression. Transgenic animals are excellent models for studying precise functions of single genes and their interactions in biological processes (CHO et al., 2009). Since the first generation of transgenic animals in 1980 (GORDON et al., 1980), there has been great improvement in the techniques, yet sometimes the transgene is not working as it is expected to be. It has been described, for example, that a transgene inserted as cDNA rather than genomic DNA may show a poorer performance (HOUDEBINE, 2002), or that the chromosomal sequences flanking the transgene have a great influence on enhancing or repressing the transgene (CRANSTON et al., 2001). The Col1(I)-AREG mouse line had been constructed with a cDNA insertion, but the transgene seems to be working, as overexpression of AREG was detected and a bone anabolic effect could be observed in two independent transgenic mouse lines. This makes the Col1(I)-AREG mouse line a suitable model for this work.

1.2. Weight and phenotype of transgenic animals

In the 8 weeks group, wild-type mice were found to be heavier. For the other age-groups no significant difference in the weight of the animals could be detected. The μ CT and pQCT examinations of the femur revealed differences in the bone phenotype between the transgenic and the wild-type mice. These examinations confirmed a specific bone phenotype for this mouse line, which was age-dependent. All the observed effects diminished with higher age (mice aged 5 months and older did not show any differences in the bone phenotype – unpublished data). This might also be an explanation for the higher weight of wild-type animals in the 8 weeks group. As the phenotype is not stable over time, the lower weight of the transgenic animals might simply be due to a transient, so far unidentified effect for this mouse

line.

1.3. Transcriptome analysis

We conducted a transcriptome analysis via microarrays to identify genes potentially involved in the high bone mass phenotype of Col1(I)-AREG mice. A GO analysis using the free online bioinformatics resource DAVID and the open source bioinformatics network Cytoscape was conducted with the obtained lists of differentially expressed genes to identify regulated genes which had been sorted into overrepresented annotation categories by these tools. Genes of interest were preferably such with an already known influence on osteoblast proliferation, and, as unpublished examinations of this transgenic mouse line also hinted to a decrease in osteoclast number, genes involved in osteoclast proliferation and differentiation. This analysis yielded results for overrepresented annotation terms mainly for biological processes concerning growth, proliferation and cell migration for the up-regulated genes of the 1 week and 4 weeks groups. A GO-analysis for the down-regulated genes could only be conducted for the 1 week group as the list for the 4 weeks group contained only 8 differentially expressed genes. No GO-analysis could be conducted for the 8 weeks group, as no differentially expressed genes were found by the microarray analysis. Additionally, the microarray analysis confirmed *Areg* overexpression for all age groups, as it could be detected in all age groups as up-regulated, although the up-regulation of *Areg* itself and the effect of it on other genes seems to be age-dependent, as in the 8 weeks group no difference of other differentially expressed genes between the transgenic and wild-type animals could be detected. Thus, there might be some certain compensatory effect of other genes in older ages. AREG is expressed in nearly all tissues of the body, and is physiologically involved in biological processes like growth, tissue repair, cell migration and apoptosis (BERASAIN & AVILA, 2014). The most distinct role that could be identified for AREG is its importance for mammary gland development, especially for mammary gland duct branching (LUETTEKE et al., 1999). This function was actually highlighted by the Cytoscape analysis for the 1 week group. Another important function of AREG has been reported in inflammation and regeneration of the liver (PARDO-SAGANTA et al., 2009). It has also been shown that mice lacking *Areg* had significantly less trabecular bone in the tibia with no differences in the midshaft of the femur (LUETTEKE et al., 1999; QIN et al., 2005). This might be because the influence of AREG on bone metabolism does not extend

to all bone compartments. A possible explanation for this effect might be the fact that AREG acts through specific EGFR homo- or heterodimers (compared to other EGFR-ligands), thus initiating specific intracellular signaling cascades (SCHNEIDER & WOLF, 2009).

As the GO-analysis of the differentially expressed genes with DAVID and Cytoscape yielded quite manageable lists of genes, some of them could be assessed individually. Some of the most prominent are discussed below, the up-regulated genes first. The majority of these up-regulated genes actually have an already known function in bone homeostasis.

SPP1 (Secreted Phosphoprotein 1), also called OPN (Osteopontin), is a phosphoprotein secreted by many cells of various tissues. In bone it is expressed by osteoblasts at various stages of differentiation and also by osteoclasts (SODEK et al., 2000). Its expression is regulated by many different hormones and growth factors, like PTH, vitamin D3, EGF, TGF- β s and many more. Additionally, it has been shown that OPN is involved in many functions during development, bone remodeling, calcification, homeostasis and immunoprotection (SODEK et al., 2000). OPN is also secreted by osteoclasts and influences osteoclast function and bone resorption (REINHOLT et al., 1990; CHELLAIAH et al., 2003). The most important function of this protein seems to be a potent inhibitory role in calcification (HUNTER et al., 1994; ZHOU et al., 2012) due to its potent ability to bind mineral crystals (SODEK et al., 2000). This gene was detected in 1 week and 4 weeks groups. *Enpp1*, another gene that has been detected as up-regulated, is known to have direct influence on the expression of *Spp1/Opn* (see below). As *Spp1* is expressed by both osteoblasts and osteoclasts, conclusions about its effects on bone formation versus bone resorption are difficult to reach.

SLIT2 is a protein which has been identified as an important factor for axon migration and stimulation, but has also inhibitory effects on axons (BROSE & TESSIER-LAVIGNE, 2000). Recently, there has also been a report describing *Slit2* expression in osteoblasts. This study revealed that, in vitro, SLIT2 inhibited the differentiation of osteoblasts (SUN et al., 2009). This gene has also been detected both in the 1 week and in the 4 weeks groups.

DCSTAMP, a seven-pass transmembrane protein, was identified as the key regulator of osteoclast cell-to-cell fusion (YAGI et al., 2005). This gene has only

been detected as differentially regulated in the 1 week group. Deletion of this gene prevents the fusion of pre-osteoclasts to the active multinucleated mature osteoclast, and DCSTAMP knockout mice were found to have higher bone mass (YAGI et al., 2005). Mice overexpressing DCSTAMP showed accelerated bone resorption and less bone mass (IWASAKI et al., 2008; CHIU et al., 2012). However, a ligand mediating these effects has not yet been detected (CHIU et al., 2012). Interestingly, this gene has been found to be up-regulated in our microarray analysis, whereas the qRT-PCR analysis revealed that the expression of this gene was unchanged in Col1(I)-AREG-transgenic mice. What one would expect is a down-regulation of this gene in the 1 week group, as the transgenic animals have a higher bone mass than the wild-type controls, and a decrease in osteoclast number was observed. The results of the qRT-PCR analysis seem to be more in accordance with the observed phenotype of the Col1(I)-AREG-transgenic mouse line than the microarray analysis result. This issue will be discussed further below.

The proteolytic enzyme MMP9 (other names: gelatinase B/type IV collagenase), only detected for the 1 week group, is expressed in osteoclasts and has an established function is the degradation of extracellular matrix in bone and in various other tissues (REPONEN et al., 1994; SUNDARAM et al., 2007). MMP9 is up-regulated by RANKL (SUNDARAM et al., 2007) and other studies revealed that TNF- α stimulated osteoblast-like MC3T3-E1 cells also express MMP9 in response to inflammatory processes (TSAI et al., 2014). Like *Dcstamp*, *Mmp9* has been detected as an up-regulated gene by our microarray analysis, but as unchanged by qRT-PCR analysis. Again, the result of the qRT-PCR seems to fit more with the phenotype of the Col1(I)-AREG-transgenic mouse line, although because of the observed decrease in osteoclast-number in this mouse line, one would rather expect a down-regulation of this gene.

Another potentially interesting gene is *Enpp1* (also known as PC-1: plasma cell membrane glycoprotein 1). It was detected in both the 1 week and the 4 weeks groups. The protein coded by this gene is an extracellular and intracellular active enzyme, which hydrolyzes phosphodiester bonds. It is expressed in many tissues of the body and in high levels in vascular smooth muscle cells, osteoblasts and chondrocytes (HUANG et al., 1994; MACKENZIE et al., 2012). This enzyme is involved indirectly in the mineralization of bones. It mainly produces inorganic pyrophosphate (PPi) by hydrolyzing ATP to AMP, and to a lesser extent inorganic

phosphate (Pi) by hydrolysis of ADP to AMP (MACKENZIE et al., 2012). PPI inhibits mineralization effectively by its capacity of binding to hydroxyapatite crystals, thus preventing further crystal growth. A decrease of extracellular PPI leads to increased mineralization by an elevated deposition of hydroxyapatites, whereas an increase of PPI results in decrease of mineralization (ADDISON et al., 2007). Additionally, there have been reports that *Enpp1* also functions as a stimulator for osteoblast differentiation, and might also be able to enhance osteoblastic gene expression (NAM et al., 2011). *Spp1/Opn*, which has also been detected as an up-regulated gene by microarray analysis (see above) is another potent mineralization inhibitor, and is influenced directly by the expression of *Enpp1*. A mouse line deficient for *Enpp1* also showed decreased *Spp1/OPN* expression (JOHNSON et al., 2003). The cooperation between *Enpp1* and *SPP1/OPN* is considered to have a synergistic effect on the inhibition of mineralization by binding hydroxyapatite (JOHNSON et al., 2003; ADDISON et al., 2007; ZHOU et al., 2012). Possibly, an up-regulation of these genes might be an indicator of the beginning of an elevated osteoclastogenesis and therefore bone resorption. But they might also be up-regulated in answer to an elevated osteoblast function.

There are two genes that had only been detected for the 4 weeks group: *Prrx1* and *Prrx2*. *Prrx* (paired-related homeobox) has been known to play a role in limb bud development (NOHNO et al., 1993; MARTIN & OLSON, 2000). More recently, a study revealed that *Prrx1b* (one of the two isoforms of *Prrx1*) and *Prrx2* mediate inhibition of osteoblast differentiation via TNF- α , by inhibition of *Runx2* and *Osx* (LU et al., 2011). TNF- α , in turn, is known to stimulate the expression of RANKL and M-CSF and therefore to initiate osteoclastogenesis (BOYCE et al., 2005; LU et al., 2011). *Prrx1* was reported to be expressed during embryonic development up to day E11.5, with much lower levels thereafter (LU et al., 2011). Interestingly, a similar effect of decreasing osteoblast differentiation via down-regulation of *Runx2* and *Osx* was reported for EGFR-signaling in bone (ZHU et al., 2011). As *Prrx1* and *Prrx2* had been found to be up-regulated in the 4 weeks group, this might be an indicator of the beginning of elevated osteoclastogenesis. This would also be in accordance with the observations for the phenotype of the *Col1(I)-AREG* mouse line, as all the observed effects in the bone phenotype disappear with increasing age.

Some of the detected genes have not been reported yet to have a specific role in bone homeostasis, but might nevertheless be interesting: Map1b (microtubule associated protein 1b) is expressed mainly in the nervous system and promotes microtubule development; its expression level is higher in childhood, than in adults (VILLARROEL-CAMPOS & GONZALEZ-BILLAULT, 2014). Cdkn2a (known under many different names like p16, INK4, ARF, among others) is a potent tumor suppressor gene (LOWE & SHERR, 2003). TIMP1 belongs to the family of tissue inhibitors of metalloproteinases. It inhibits matrix-metalloproteinases like, for example, MMP9, and it promotes the proliferation of several different cell types (RIES, 2014).

For the differentially expressed down-regulated genes for the 1 week group, the GO-analysis yielded results in the categories hematopoiesis and immune system development. There had been no reports for *Areg* influencing the development of hematopoietic or immune cells so far (BERASAIN & AVILA, 2014). Only one of the detected up-regulated genes, *Cdkn2a/p16*, was reported to possibly influence the physiologic quiescence of hematopoietic stem cells (EZOE et al., 2004). This might explain the detection of the down-regulation of genes concerning hematopoiesis. As this effect could only be observed for the 1 week group (the list of differentially expressed down-regulated genes for the 4 weeks group contained only very few genes), it may simply represent a transient effect.

When assessing these in parts contradictory results from our transcriptome analysis, the reliability of the used technology has also to be taken into account. Our transcriptome analysis was conducted via microarrays, whose principle is hybridization of the transcript of the isolated RNA to a “probe” immobilized on the microarray chip. However, this method is not infallible. In fact, there is a number of error sources which can affect the obtained results. There are for example cross hybridizations between similar sequences, high signal-to-noise ratios, which leads to the problem that lowly expressed genes might not be detected, or conversely, hybridization saturation which prevents an accurate detection of highly expressed genes (HURD & NELSON, 2009; SIRBU et al., 2012). These error sources might either lead to false positive or false negative signals, which have great influence on the obtained results. Regarding the different results obtained with microarray analysis and qRT-PCR, the question is which results are more reliable. In many experiments, qRT-PCR is used for validation of microarray analysis, because of the

high sensitivity to quantify genes (STANTON, 2001; WONG & MEDRANO, 2005; SHI et al., 2006). Although the transcriptome analysis via microarray has been criticized for its sometimes poor reproducibility, a quality analysis project indicated a satisfactory correlation between the results of different microarray platforms and other gene expression technologies, like TaqMan (SHI et al., 2006), even if the correlation is never perfect. Thus, it might be simply a coincidence that false positive genes (*Dcstamp* and *Mmp9*) were selected for qRT-PCR. Because of the higher sensitivity of qRT-PCR and the phenotype of the Col1(I)-AREG mouse line, it seems more likely that the qRT-PCR results are the genuine ones.

Our analysis revealed that the effect of AREG overexpression on the osteoblast transcriptome is definitively age-dependent, which is in accordance with the phenotype of this mouse line. What are the explanations for this phenomenon? Our microarray analysis revealed that genes involved in osteoclastogenesis, such as *Dcstamp* and *Mmp9* are up-regulated, though these results could not be confirmed by the qRT-PCR analysis. The levels of *Rankl* and *Opg* have been detected by qRT-PCR to be unchanged for the transgenic mice of the 1 week group in comparison to the wild-types. To detect a regulation of genes involved in osteoclastogenesis would have been particularly interesting. On the one hand, because of the observed phenotype for this mouse line (decreased number of osteoclasts), and on the other hand, because it has been described, that genes involved in osteoclastogenesis are paradoxically up-regulated with an anabolic PTH regime (KOH et al., 2005; LI et al., 2007a; LI et al., 2007b). A study examining the gene expression of continuous (catabolic effect) or intermittent (anabolic effect) PTH treatment identified a down-regulation of *Opg*, and an up-regulation of *Rankl* as a response to intermittent PTH treatment (LI et al., 2007a). Interestingly, the same study found, that continuous PTH treatment (catabolic regime) did not increase the stimulation of genes involved in osteoclastogenesis (LI et al., 2007a). It has been described, that activation of the EGFR in bone leads to a decrease of OPG, therefore inducing an unbalance between RANKL and OPG in favor for RANKL and leading to increased osteoclastogenesis (ZHU et al., 2007; LYNCH, 2011). The ratio RANKL/OPG has been described to be more relevant for osteoclastogenesis than total levels of up- or down-regulation for each gene (LI et al., 2007a). Interestingly, OPG has been found to be an inhibitor of the anabolic function of PTH (KOH et al., 2005), although it is the antagonist of RANKL, a stimulator of osteoclastogenesis.

Our results confirm a bone anabolic effect of *Areg* via the EGFR, yet this effect seems to be compensated by unknown mechanisms with increasing age. Furthermore, an alteration of the expression of genes regulating osteoclastogenesis mediated by bone specific up-regulation of *Areg* could not be satisfactorily proven. The mechanism behind the age-dependent anabolic function of *Areg* on bone will need further investigation. The Col1(I)-AREG mouse line exhibits a permanent up-regulation of *Areg*, but an anabolic function with PTH treatment is only achieved when PTH is given intermittently. This might possibly be the reason why the effect of an initially higher bone mass of this mouse line disappears with increased age. A possible explanation might be the involvement of a feedback or rebound loop, as is known for several other biological processes mediated by hormones, like, for example, the ovarian cycle (MESSINIS, 2006). As these results were obtained via microarray analysis, and this technology has a number of limitations, it seems to be worth to examine the effects in this transgenic mouse line with newer and more sensitive methods for all age-groups. The method of choice would be an analysis with the new RNA-Seq technology (Next or Second Generation Sequencing). RNA-Seq has many advantages in comparison to the microarray technology. This new technology is becoming increasingly affordable and would currently be the technology of choice for transcriptome analyses. Unlike microarrays, RNA-Seq works without hybridization, which is, as mentioned above, a major source for various errors. In contrast, the isolated RNA is sequenced directly by RNA-Seq, and the reads are counted (WANG et al., 2009). This method has other additional advantages compared to microarrays: No known compatible sequence is needed for the detection of transcripts, and RNA-Seq has a higher dynamic range in detecting transcripts either with a very high or low expression rate (WANG et al., 2009).

1.4. Final considerations

Areg is a very interesting gene whose role in bone metabolism deserves further studies. It definitively promotes bone anabolism, yet its effect seems to be age-dependent. Our analysis revealed that genes involved in bone homeostasis, like *Slit2*, *Enpp1*, *Spp1/Opn*, and some others, are regulated as a consequence of *Areg*-up-regulation. Several genes regulating osteoclastogenesis have been detected via microarrays to be regulated by an osteoblast-specific overexpression of *Areg*, though not by qRT-PCR for the 1 week group. Intermittent PTH treatment has been reported to promote an up-regulation of genes involved in osteoclastogenesis

(LI et al., 2007a). Whether *Areg* also has an effect on genes involved in osteoclastogenesis, could not be terminally verified, as our results were ambiguous. The paradoxical finding of an up-regulation of genes promoting osteoclastogenesis along with an anabolic effect on bone is a very interesting observation. As this transcriptome study could not ultimately clarify the role of *Areg* in influencing the genes involved in osteoclastogenesis, further examinations with newer and more sensitive methods will be needed.

VI. ZUSAMMENFASSUNG

Osteoporose ist eine schwerwiegende Erkrankung, die rund ein Drittel aller postmenopausalen Frauen betrifft und auf Grund der erhöhten Frakturrate zu einer Verminderung der Lebensqualität der Betroffenen führt. PTH ist derzeit das einzig verfügbare Medikament für die Behandlung von Osteoporose mit anaboler Wirkung auf den Knochenaufbau. Der Wirkmechanismus ist bis heute ungeklärt. *Areg*, ein Ligand des EGFR, konnte als eines der Gene identifiziert werden, die durch PTH-Behandlung hochreguliert werden (QIN et al., 2005). Eine neue transgene Mauslinie, die *Col1(I)-AREG*-Linie, wurde generiert, um den Effekt von AREG auf den Knochenstoffwechsel untersuchen zu können. Diese Mauslinie zeichnet sich durch eine Osteoblasten-spezifische Überexpression von AREG aus. μ CT und pQCT Untersuchungen bestätigten eine signifikante Erhöhung der totalen Knochendichte des Femurs. Aus diesem Grund wurde eine Analyse des Transkriptoms für diese Mauslinie mittels Microarrays durchgeführt, mit dem Ziel, Abweichungen in der Genexpression zu entdecken, die dazu beitragen könnten, diesen knochenanabolen Effekt von *Areg* aufdecken zu können. Für die Analyse des Transkriptoms wurden drei Altersgruppen gewählt: 1 Woche (neugeborene Mäuse), 4 Wochen (jugendliche Mäuse) und 8 Wochen (ausgewachsene Mäuse). Abweichungen in der Genexpression waren am stärksten nachweisbar für die 1 Wochen-Gruppe mit 47 hoch-, und 187 runterregulierten Genen. Mit steigendem Alter nahmen diese Abweichungen ab. Für die 4 Wochen-Gruppe waren 8 runter- und 56 hochregulierte Gene nachweisbar und für die 8 Wochen-Gruppe waren keine differentiell exprimierten Gene mehr nachweisbar. Die Listen der differentiell exprimierten Gene wurden mittels GO-Analyse untersucht, um nach überrepräsentierten Kategorien für diese Gene zu suchen und deren Zusammenhänge bildlich darstellen zu können. Unter den differentiell hochexprimierten Genen, für die bereits eine Funktion im Knochenstoffwechsel bekannt war, waren zum Beispiel *Slit2*, *Enpp1*, *Spp1/Opn* sowohl für die 1 Wochen- als auch für die 4 Wochen-Gruppe, und *Dcstamp* und *Mmp9* lediglich für die 1 Wochen-Gruppe. Diese Ergebnisse konnten mittels der zusätzlich für die 1 Wochen-Gruppe durchgeführte qRT-PCR-Analyse nicht bestätigt werden: keines der untersuchten Gene (*Dcstamp*, *Mmp9*, *Opg*, *Rankl*) war statistisch signifikant reguliert. Es wurde beschrieben, dass Gene, die die Osteoklastogenese

vermitteln, durch intermittierende (also anabole) PTH-Behandlung hochreguliert werden (LI et al., 2007a). Wir konnten einen Einfluss der Osteoblasten-spezifischen Überexprimierung von *Areg* auf die Regulierung entsprechender Gene nicht nachweisen, da sich die Ergebnisse der Microarrays und der qRT-PCR widersprachen. Es erscheint daher lohnend, den Einfluss von *Areg* auf den Knochenstoffwechsel mit neueren und sensitiveren Methoden wie RNA-Seq zu untersuchen.

VII. SUMMARY

Osteoporosis is a severe disease that affects around 1/3 of postmenopausal women and leads to an impaired quality of life, mainly due to an increased fracture rate. PTH is currently the only anabolic agent used for the treatment of osteoporosis. It remains unknown how this effect is mediated. *Areg*, a ligand of the epidermal growth factor receptor (EGFR) has been identified as a PTH target gene (QIN et al., 2005). A new transgenic mouse line, the Col1(I)-AREG mouse line, had been generated to examine the effect of AREG on bone homeostasis. This mouse line exhibits an osteoblast-specific over-expression of AREG. μ CT and pQCT revealed a significant increase in total bone mineral density of the femur. Therefore, to examine alterations of gene expression that might help unravel this mechanism of an anabolic effect on bone by Areg, we conducted a bone transcriptome analysis using microarrays. Three age groups had been chosen for the transcriptome analysis: 1 week (newborn), 4 weeks (adolescent) and 8 weeks (adult). Gene expression alterations were highest in the 1 week group with 184 down-regulated genes and 47 up-regulated genes, and decreased with age with 8 down-regulated genes and 56 up-regulated genes in the 4 weeks group, and no detectable differentially expressed genes in the 8 weeks group. Lists of differentially expressed genes were then analyzed with a GO-analysis to search for overrepresented annotation terms and visualize the connections of the differentially expressed genes. Prominent genes among the differentially expressed up-regulated genes, with a known function in bone homeostasis were for example *Slit2*, *Enpp1*, *Spp1/Opn* for 1 week and 4 weeks groups and *Dcstamp* and *Mmp9* only for the 1 week group. qRT-PCR, conducted only for the 1 week group, unfortunately did not confirm the results obtained by our microarray analysis: none of the examined genes (*Dcstamp*, *Mmp9*, *Opg*, *Rankl*) had been detected as significantly regulated. Genes involved in osteoclastogenesis had been reported to be up-regulated by an intermittent PTH treatment (LI et al., 2007a). We were not able to verify an effect of the osteoblast-specific up-regulation of *Areg* on the regulation of these genes, because the results of microarray and qRT-PCR analysis were ambiguous. Therefore, it seems worth to examine the role of *Areg* in bone homeostasis with newer and more sensitive methods like RNA-Seq.

VIII. BIBLIOGRAPHY

Addison WN, Azari F, Sorensen ES, Kaartinen MT, McKee MD. Pyrophosphate inhibits mineralization of osteoblast cultures by binding to mineral, up-regulating osteopontin, and inhibiting alkaline phosphatase activity. *J Biol Chem* 2007; 282: 15872-83.

Ashburner M, Ball CA, Blake JA, Botstein D, Butler H, Cherry JM, Davis AP, Dolinski K, Dwight SS, Eppig JT, Harris MA, Hill DP, Issel-Tarver L, Kasarskis A, Lewis S, Matese JC, Richardson JE, Ringwald M, Rubin GM, Sherlock G. Gene ontology: tool for the unification of biology. The Gene Ontology Consortium. *Nat Genet* 2000; 25: 25-9.

Aubin JE. Bone stem cells. *J Cell Biochem Suppl* 1998; 30-31: 73-82.

Berasain C, Avila MA. Amphiregulin. *Semin Cell Dev Biol* 2014; 28: 31-41.

Bindea G, Mlecnik B, Hackl H, Charoentong P, Tosolini M, Kirilovsky A, Fridman WH, Pages F, Trajanoski Z, Galon J. ClueGO: a Cytoscape plug-in to decipher functionally grouped gene ontology and pathway annotation networks. *Bioinformatics* 2009; 25: 1091-3.

Bindea G, Galon J, Mlecnik B. CluePedia Cytoscape plugin: pathway insights using integrated experimental and in silico data. *Bioinformatics* 2013; 29: 661-3.

Bone HG, Bolognese MA, Yuen CK, Kendler DL, Miller PD, Yang YC, Grazette L, San Martin J, Gallagher JC. Effects of denosumab treatment and discontinuation on bone mineral density and bone turnover markers in postmenopausal women with low bone mass. *J Clin Endocrinol Metab* 2011; 96: 972-80.

Bonewald LF. The amazing osteocyte. *J Bone Miner Res* 2011; 26: 229-38.

Boyce BF, Li P, Yao Z, Zhang Q, Badell IR, Schwarz EM, O'Keefe RJ, Xing L. TNF-alpha and pathologic bone resorption. *Keio J Med* 2005; 54: 127-31.

Brose K, Tessier-Lavigne M. Slit proteins: key regulators of axon guidance, axonal branching, and cell migration. *Curr Opin Neurobiol* 2000; 10: 95-102.

Canalis E, Raisz LG. Effect of epidermal growth factor on bone formation in vitro. *Endocrinology* 1979; 104: 862-9.

Canalis E. New treatment modalities in osteoporosis. *Endocr Pract* 2010; 16: 855-63.

Canalis E. Wnt signalling in osteoporosis: mechanisms and novel therapeutic approaches. *Nat Rev Endocrinol* 2013; 9: 575-83.

Chan SY, Wong RW. Expression of epidermal growth factor in transgenic mice causes growth retardation. *J Biol Chem* 2000; 275: 38693-8.

Chellaiah MA, Kizer N, Biswas R, Alvarez U, Strauss-Schoenberger J, Rifas L, Rittling SR, Denhardt DT, Hruska KA. Osteopontin deficiency produces osteoclast dysfunction due to reduced CD44 surface expression. *Mol Biol Cell* 2003; 14: 173-89.

Chien HH, Lin WL, Cho MI. Down-regulation of osteoblastic cell differentiation by epidermal growth factor receptor. *Calcif Tissue Int* 2000; 67: 141-50.

Chiu YH, Mensah KA, Schwarz EM, Ju Y, Takahata M, Feng C, McMahon LA, Hicks DG, Panepento B, Keng PC, Ritchlin CT. Regulation of human osteoclast development by dendritic cell-specific transmembrane protein (DC-STAMP). *J Bone Miner Res* 2012; 27: 79-92.

Cho A, Haruyama N, Kulkarni AB. Generation of transgenic mice. *Curr Protoc Cell Biol* 2009; Chapter 19: Unit 19 1.

Citri A, Yarden Y. EGF-ERBB signalling: towards the systems level. *Nat Rev Mol Cell Biol* 2006; 7: 505-16.

Claxton AJ, Cramer J, Pierce C. A systematic review of the associations between dose regimens and medication compliance. *Clin Ther* 2001; 23: 1296-310.

conference Cd. Consensus development conference: diagnosis, prophylaxis, and treatment of osteoporosis. *Am J Med* 1993; 94: 646-50.

Conner DA. Transgenic mouse production by zygote injection. *Curr Protoc Mol Biol* 2004; Chapter 23: Unit 23 9.

Cranston A, Dong C, Howcroft J, Clark AJ. Chromosomal sequences flanking an efficiently expressed transgene dramatically enhance its expression. *Gene* 2001; 269: 217-25.

Dacquin R, Starbuck M, Schinke T, Karsenty G. Mouse alpha1(I)-collagen promoter is the best known promoter to drive efficient Cre recombinase expression in osteoblast. *Dev Dyn* 2002; 224: 245-51.

Dennis G, Jr., Sherman BT, Hosack DA, Yang J, Gao W, Lane HC, Lempicki RA. DAVID: Database for Annotation, Visualization, and Integrated Discovery. *Genome Biol* 2003; 4: P3.

Dennison E, Mohamed MA, Cooper C. Epidemiology of osteoporosis. *Rheum Dis Clin North Am* 2006; 32: 617-29.

Dobnig H, Turner RT. Evidence that intermittent treatment with parathyroid hormone increases bone formation in adult rats by activation of bone lining cells. *Endocrinology* 1995; 136: 3632-8.

Ducy P, Schinke T, Karsenty G. The osteoblast: a sophisticated fibroblast under central surveillance. *Science* 2000; 289: 1501-4.

Erickson SL, O'Shea KS, Ghaboosi N, Loverro L, Frantz G, Bauer M, Lu LH, Moore MW. ErbB3 is required for normal cerebellar and cardiac development: a

comparison with ErbB2-and heregulin-deficient mice. *Development* 1997; 124: 4999-5011.

Eriksen EF, Diez-Perez A, Boonen S. Update on long-term treatment with bisphosphonates for postmenopausal osteoporosis: a systematic review. *Bone* 2014; 58: 126-35.

Ezoe S, Matsumura I, Satoh Y, Tanaka H, Kanakura Y. Cell cycle regulation in hematopoietic stem/progenitor cells. *Cell Cycle* 2004; 3: 314-8.

Fang MA, Kujubu DA, Hahn TJ. The effects of prostaglandin E2, parathyroid hormone, and epidermal growth factor on mitogenesis, signaling, and primary response genes in UMR 106-01 osteoblast-like cells. *Endocrinology* 1992; 131: 2113-9.

Felix R, Cecchini MG, Fleisch H. Macrophage colony stimulating factor restores in vivo bone resorption in the op/op osteopetrotic mouse. *Endocrinology* 1990; 127: 2592-4.

Fujikawa Y, Quinn JM, Sabokbar A, McGee JO, Athanasou NA. The human osteoclast precursor circulates in the monocyte fraction. *Endocrinology* 1996; 137: 4058-60.

Gassmann M, Casagrande F, Orioli D, Simon H, Lai C, Klein R, Lemke G. Aberrant neural and cardiac development in mice lacking the ErbB4 neuregulin receptor. *Nature* 1995; 378: 390-4.

Gordon JW, Scangos GA, Plotkin DJ, Barbosa JA, Ruddle FH. Genetic transformation of mouse embryos by microinjection of purified DNA. *Proc Natl Acad Sci U S A* 1980; 77: 7380-4.

Gunness-Hey M, Hock JM. Increased trabecular bone mass in rats treated with human synthetic parathyroid hormone. *Metab Bone Dis Relat Res* 1984; 5: 177-81.

Harris RC, Chung E, Coffey RJ. EGF receptor ligands. *Exp Cell Res* 2003; 284: 2-13.

Haruyama N, Cho A, Kulkarni AB. Overview: engineering transgenic constructs and mice. *Curr Protoc Cell Biol* 2009; Chapter 19: Unit 19 0.

Hata R, Hori H, Nagai Y, Tanaka S, Kondo M, Hiramatsu M, Utsumi N, Kumegawa M. Selective inhibition of type I collagen synthesis in osteoblastic cells by epidermal growth factor. *Endocrinology* 1984; 115: 867-76.

Hernlund E, Svedbom A, Ivergard M, Compston J, Cooper C, Stenmark J, McCloskey EV, Jonsson B, Kanis JA. Osteoporosis in the European Union: medical management, epidemiology and economic burden. A report prepared in collaboration with the International Osteoporosis Foundation (IOF) and the European Federation of Pharmaceutical Industry Associations (EFPIA). *Arch Osteoporos* 2013; 8: 136.

Herrero J, Valencia A, Dopazo J. A hierarchical unsupervised growing neural network for clustering gene expression patterns. *Bioinformatics* 2001; 17: 126-36.

Holbro T, Hynes NE. ErbB receptors: directing key signaling networks throughout life. *Annu Rev Pharmacol Toxicol* 2004; 44: 195-217.

Houdebine LM. The methods to generate transgenic animals and to control transgene expression. *J Biotechnol* 2002; 98: 145-60.

<http://www.genomics.agilent.com/en/home.jsp>.

<http://www.iofbonehealth.org/>.

Huang R, Rosenbach M, Vaughn R, Provvedini D, Rebbe N, Hickman S, Goding J, Terkeltaub R. Expression of the murine plasma cell nucleotide pyrophosphohydrolase PC-1 is shared by human liver, bone, and cartilage cells.

Regulation of PC-1 expression in osteosarcoma cells by transforming growth factor-beta. *J Clin Invest* 1994; 94: 560-7.

Huber W, von Heydebreck A, Sultmann H, Poustka A, Vingron M. Variance stabilization applied to microarray data calibration and to the quantification of differential expression. *Bioinformatics* 2002; 18 Suppl 1: S96-104.

Hunter GK, Kyle CL, Goldberg HA. Modulation of crystal formation by bone phosphoproteins: structural specificity of the osteopontin-mediated inhibition of hydroxyapatite formation. *Biochem J* 1994; 300 (Pt 3): 723-8.

Hurd PJ, Nelson CJ. Advantages of next-generation sequencing versus the microarray in epigenetic research. *Brief Funct Genomic Proteomic* 2009; 8: 174-83.

Huybrechts KF, Ishak KJ, Caro JJ. Assessment of compliance with osteoporosis treatment and its consequences in a managed care population. *Bone* 2006; 38: 922-8.

Iwasaki R, Ninomiya K, Miyamoto K, Suzuki T, Sato Y, Kawana H, Nakagawa T, Suda T, Miyamoto T. Cell fusion in osteoclasts plays a critical role in controlling bone mass and osteoblastic activity. *Biochem Biophys Res Commun* 2008; 377: 899-904.

Jhappan C, Stahle C, Harkins RN, Fausto N, Smith GH, Merlino GT. TGF alpha overexpression in transgenic mice induces liver neoplasia and abnormal development of the mammary gland and pancreas. *Cell* 1990; 61: 1137-46.

John M. Eisenberg Center for Clinical Decisions and Communications Science (2007) Treatment To Prevent Osteoporotic Fractures: An Update

Comparative Effectiveness Review Summary Guides for Clinicians, Rockville MD

Johnell O, Kanis J. Epidemiology of osteoporotic fractures. *Osteoporos Int* 2005;

16 Suppl 2: S3-7.

Johnson K, Goding J, Van Etten D, Sali A, Hu SI, Farley D, Krug H, Hessle L, Millan JL, Terkeltaub R. Linked deficiencies in extracellular PP(i) and osteopontin mediate pathologic calcification associated with defective PC-1 and ANK expression. *J Bone Miner Res* 2003; 18: 994-1004.

Kanehisa M. The KEGG database. *Novartis Found Symp* 2002; 247: 91-101; discussion -3, 19-28, 244-52.

Kanis JA, McCloskey EV, Johansson H, Oden A, Melton LJ, 3rd, Khaltsev N. A reference standard for the description of osteoporosis. *Bone* 2008; 42: 467-75.

Karsenty G, Wagner EF. Reaching a genetic and molecular understanding of skeletal development. *Dev Cell* 2002; 2: 389-406.

Koh AJ, Demiralp B, Neiva KG, Hooten J, Nohutcu RM, Shim H, Datta NS, Taichman RS, McCauley LK. Cells of the osteoclast lineage as mediators of the anabolic actions of parathyroid hormone in bone. *Endocrinology* 2005; 146: 4584-96.

Kumegawa M, Hiramatsu M, Hatakeyama K, Yajima T, Kodama H, Osaki T, Kurisu K. Effects of epidermal growth factor on osteoblastic cells in vitro. *Calcif Tissue Int* 1983; 35: 542-8.

Lee KF, Simon H, Chen H, Bates B, Hung MC, Hauser C. Requirement for neuregulin receptor erbB2 in neural and cardiac development. *Nature* 1995; 378: 394-8.

Li X, Liu H, Qin L, Tamasi J, Bergenstock M, Shapses S, Feyen JH, Notterman DA, Partridge NC. Determination of dual effects of parathyroid hormone on skeletal gene expression in vivo by microarray and network analysis. *J Biol Chem* 2007a; 282: 33086-97.

Li X, Qin L, Bergenstock M, Bevelock LM, Novack DV, Partridge NC. Parathyroid hormone stimulates osteoblastic expression of MCP-1 to recruit and increase the fusion of pre/osteoclasts. *J Biol Chem* 2007b; 282: 33098-106.

Liu C, Xie W, Gui C, Du Y. Pronuclear microinjection and oviduct transfer procedures for transgenic mouse production. *Methods Mol Biol* 2013; 1027: 217-32.

Lockhart DJ, Winzeler EA. Genomics, gene expression and DNA arrays. *Nature* 2000; 405: 827-36.

Long F. Building strong bones: molecular regulation of the osteoblast lineage. *Nat Rev Mol Cell Biol* 2012; 13: 27-38.

Lowe SW, Sherr CJ. Tumor suppression by Ink4a-Arf: progress and puzzles. *Curr Opin Genet Dev* 2003; 13: 77-83.

Loza J, Carpio L, Lawless G, Marzec N, Dziak R. Role of extracellular calcium influx in EGF-induced osteoblastic cell proliferation. *Bone* 1995; 16: 341S-7S.

Lu X, Beck GR, Jr., Gilbert LC, Camalier CE, Bateman NW, Hood BL, Conrads TP, Kern MJ, You S, Chen H, Nanes MS. Identification of the homeobox protein Prx1 (MHox, Prrx-1) as a regulator of osterix expression and mediator of tumor necrosis factor alpha action in osteoblast differentiation. *J Bone Miner Res* 2011; 26: 209-19.

Luetkeke NC, Qiu TH, Fenton SE, Troyer KL, Riedel RF, Chang A, Lee DC. Targeted inactivation of the EGF and amphiregulin genes reveals distinct roles for EGF receptor ligands in mouse mammary gland development. *Development* 1999; 126: 2739-50.

Lynch CC. Matrix metalloproteinases as master regulators of the vicious cycle of bone metastasis. *Bone* 2011; 48: 44-53.

Mackenzie NC, Huesa C, Rutsch F, MacRae VE. New insights into NPP1 function: lessons from clinical and animal studies. *Bone* 2012; 51: 961-8.

Martin JF, Olson EN. Identification of a prx1 limb enhancer. *Genesis* 2000; 26: 225-9.

McGreevy C, Williams D. Safety of drugs used in the treatment of osteoporosis. *Ther Adv Drug Saf* 2011; 2: 159-72.

Messinis IE. Ovarian feedback, mechanism of action and possible clinical implications. *Hum Reprod Update* 2006; 12: 557-71.

Miettinen PJ, Berger JE, Meneses J, Phung Y, Pedersen RA, Werb Z, Derynck R. Epithelial immaturity and multiorgan failure in mice lacking epidermal growth factor receptor. *Nature* 1995; 376: 337-41.

Miettinen PJ, Chin JR, Shum L, Slavkin HC, Shuler CF, Derynck R, Werb Z. Epidermal growth factor receptor function is necessary for normal craniofacial development and palate closure. *Nat Genet* 1999; 22: 69-73.

Mundy GR, Guise TA. Hormonal control of calcium homeostasis. *Clin Chem* 1999; 45: 1347-52.

Nakagawa N, Kinoshita M, Yamaguchi K, Shima N, Yasuda H, Yano K, Morinaga T, Higashio K. RANK is the essential signaling receptor for osteoclast differentiation factor in osteoclastogenesis. *Biochem Biophys Res Commun* 1998; 253: 395-400.

Nam HK, Liu J, Li Y, Kragor A, Hatch NE. Ectonucleotide pyrophosphatase/phosphodiesterase-1 (ENPP1) protein regulates osteoblast differentiation. *J Biol Chem* 2011; 286: 39059-71.

Neer RM, Arnaud CD, Zanchetta JR, Prince R, Gaich GA, Reginster JY, Hodsman

AB, Eriksen EF, Ish-Shalom S, Genant HK, Wang O, Mitlak BH. Effect of parathyroid hormone (1-34) on fractures and bone mineral density in postmenopausal women with osteoporosis. *N Engl J Med* 2001; 344: 1434-41.

Ng KW, Partridge NC, Niall M, Martin TJ. Stimulation of DNA synthesis by epidermal growth factor in osteoblast-like cells. *Calcif Tissue Int* 1983; 35: 624-8.

Nohno T, Koyama E, Myokai F, Taniguchi S, Ohuchi H, Saito T, Noji S. A chicken homeobox gene related to *Drosophila* paired is predominantly expressed in the developing limb. *Dev Biol* 1993; 158: 254-64.

Oda K, Matsuoka Y, Funahashi A, Kitano H. A comprehensive pathway map of epidermal growth factor receptor signaling. *Mol Syst Biol* 2005; 1: 2005 0010.

Olayioye MA, Neve RM, Lane HA, Hynes NE. The ErbB signaling network: receptor heterodimerization in development and cancer. *EMBO J* 2000; 19: 3159-67.

Olsen BR, Reginato AM, Wang W. Bone development. *Annu Rev Cell Dev Biol* 2000; 16: 191-220.

Pardo-Saganta A, Latasa MU, Castillo J, Alvarez-Asiain L, Perugorria MJ, Sarobe P, Rodriguez-Ortigosa CM, Prieto J, Berasain C, Santamaria M, Avila MA. The epidermal growth factor receptor ligand amphiregulin is a negative regulator of hepatic acute-phase gene expression. *J Hepatol* 2009; 51: 1010-20.

Poole KE, Reeve J. Parathyroid hormone - a bone anabolic and catabolic agent. *Curr Opin Pharmacol* 2005; 5: 612-7.

Provenzano AP, Besner GE, James PF, Harding PA. Heparin-binding EGF-like growth factor (HB-EGF) overexpression in transgenic mice downregulates insulin-like growth factor binding protein (IGFBP)-3 and -4 mRNA. *Growth Factors* 2005; 23: 19-31.

Qin L, Qiu P, Wang L, Li X, Swarthout JT, Soteropoulos P, Tolia P, Partridge NC. Gene expression profiles and transcription factors involved in parathyroid hormone signaling in osteoblasts revealed by microarray and bioinformatics. *J Biol Chem* 2003; 278: 19723-31.

Qin L, Partridge NC. Stimulation of amphiregulin expression in osteoblastic cells by parathyroid hormone requires the protein kinase A and cAMP response element-binding protein signaling pathway. *J Cell Biochem* 2005; 96: 632-40.

Qin L, Tamasi J, Raggatt L, Li X, Feyen JH, Lee DC, Diccico-Bloom E, Partridge NC. Amphiregulin is a novel growth factor involved in normal bone development and in the cellular response to parathyroid hormone stimulation. *J Biol Chem* 2005; 280: 3974-81.

Reinholt FP, Hultenby K, Oldberg A, Heinegard D. Osteopontin--a possible anchor of osteoclasts to bone. *Proc Natl Acad Sci U S A* 1990; 87: 4473-5.

Reponen P, Sahlberg C, Munaut C, Thesleff I, Tryggvason K. High expression of 92-kD type IV collagenase (gelatinase B) in the osteoclast lineage during mouse development. *J Cell Biol* 1994; 124: 1091-102.

Ries C. Cytokine functions of TIMP-1. *Cell Mol Life Sci* 2014; 71: 659-72.

Riggs BL, Khosla S, Melton LJ, 3rd. Sex steroids and the construction and conservation of the adult skeleton. *Endocr Rev* 2002; 23: 279-302.

Rubin KH, Abrahamsen B, Friis-Holmberg T, Hjelmberg JV, Bech M, Hermann AP, Barkmann R, Gluer CC, Brixen K. Comparison of different screening tools (FRAX(R), OST, ORAI, OSIRIS, SCORE and age alone) to identify women with increased risk of fracture. A population-based prospective study. *Bone* 2013; 56: 16-22.

Sabbieti MG, Agas D, Xiao L, Marchetti L, Coffin JD, Doetschman T, Hurley MM.

Endogenous FGF-2 is critically important in PTH anabolic effects on bone. *J Cell Physiol* 2009; 219: 143-51.

Sambrook P, Cooper C. Osteoporosis. *Lancet* 2006; 367: 2010-8.

Sandgren EP, Luetkeke NC, Palmiter RD, Brinster RL, Lee DC. Overexpression of TGF alpha in transgenic mice: induction of epithelial hyperplasia, pancreatic metaplasia, and carcinoma of the breast. *Cell* 1990; 61: 1121-35.

Schena M, Shalon D, Davis RW, Brown PO. Quantitative monitoring of gene expression patterns with a complementary DNA microarray. *Science* 1995; 270: 467-70.

Schmittgen TD, Livak KJ. Analyzing real-time PCR data by the comparative C(T) method. *Nat Protoc* 2008; 3: 1101-8.

Schneider MR, Mayer-Roenne B, Dahlhoff M, Proell V, Weber K, Wolf E, Erben RG. High cortical bone mass phenotype in betacellulin transgenic mice is EGFR dependent. *J Bone Miner Res* 2009a; 24: 455-67.

Schneider MR, Sibilio M, Erben RG. The EGFR network in bone biology and pathology. *Trends Endocrinol Metab* 2009b; 20: 517-24.

Schneider MR, Wolf E. The epidermal growth factor receptor ligands at a glance. *J Cell Physiol* 2009; 218: 460-6.

Schneider MR, Dahlhoff M, Andrukhova O, Grill J, Glosmann M, Schuler C, Weber K, Wolf E, Erben RG. Normal epidermal growth factor receptor signaling is dispensable for bone anabolic effects of parathyroid hormone. *Bone* 2012; 50: 237-44.

Schulze A, Downward J. Navigating gene expression using microarrays--a technology review. *Nat Cell Biol* 2001; 3: E190-5.

Shannon P, Markiel A, Ozier O, Baliga NS, Wang JT, Ramage D, Amin N, Schwikowski B, Ideker T. Cytoscape: a software environment for integrated models of biomolecular interaction networks. *Genome Res* 2003; 13: 2498-504.

Shi L, Reid LH, Jones WD, Shippy R, Warrington JA, Baker SC, Collins PJ, de Longueville F, Kawasaki ES, Lee KY, Luo Y, Sun YA, Willey JC, Setterquist RA, Fischer GM, Tong W, Dragan YP, Dix DJ, Frueh FW, Goodsaid FM, Herman D, Jensen RV, Johnson CD, Lobenhofer EK, Puri RK, Schrf U, Thierry-Mieg J, Wang C, Wilson M, Wolber PK, Zhang L, Amur S, Bao W, Barbacioru CC, Lucas AB, Bertholet V, Boysen C, Bromley B, Brown D, Brunner A, Canales R, Cao XM, Cebula TA, Chen JJ, Cheng J, Chu TM, Chudin E, Corson J, Corton JC, Croner LJ, Davies C, Davison TS, Delenstarr G, Deng X, Dorris D, Eklund AC, Fan XH, Fang H, Fulmer-Smentek S, Fuscoe JC, Gallagher K, Ge W, Guo L, Guo X, Hager J, Haje PK, Han J, Han T, Harbottle HC, Harris SC, Hatchwell E, Hauser CA, Hester S, Hong H, Hurban P, Jackson SA, Ji H, Knight CR, Kuo WP, LeClerc JE, Levy S, Li QZ, Liu C, Liu Y, Lombardi MJ, Ma Y, Magnuson SR, Maqsodi B, McDaniel T, Mei N, Myklebost O, Ning B, Novoradovskaya N, Orr MS, Osborn TW, Papallo A, Patterson TA, Perkins RG, Peters EH, Peterson R, Philips KL, Pine PS, Pusztai L, Qian F, Ren H, Rosen M, Rosenzweig BA, Samaha RR, Schena M, Schroth GP, Shchegrova S, Smith DD, Staedtler F, Su Z, Sun H, Szallasi Z, Tezak Z, Thierry-Mieg D, Thompson KL, Tikhonova I, Turpaz Y, Vallanat B, Van C, Walker SJ, Wang SJ, Wang Y, Wolfinger R, Wong A, Wu J, Xiao C, Xie Q, Xu J, Yang W, Zhang L, Zhong S, Zong Y, Slikker W, Jr. The MicroArray Quality Control (MAQC) project shows inter- and intraplatform reproducibility of gene expression measurements. *Nat Biotechnol* 2006; 24: 1151-61.

Sibilia M, Wagner EF. Strain-dependent epithelial defects in mice lacking the EGF receptor. *Science* 1995; 269: 234-8.

Sibilia M, Wagner B, Hoebertz A, Elliott C, Marino S, Jochum W, Wagner EF. Mice humanised for the EGF receptor display hypomorphic phenotypes in skin, bone and heart. *Development* 2003; 130: 4515-25.

Simonet WS, Lacey DL, Dunstan CR, Kelley M, Chang MS, Luthy R, Nguyen HQ,

Wooden S, Bennett L, Boone T, Shimamoto G, DeRose M, Elliott R, Colombero A, Tan HL, Trail G, Sullivan J, Davy E, Bucay N, Renshaw-Gegg L, Hughes TM, Hill D, Pattison W, Campbell P, Sander S, Van G, Tarpley J, Derby P, Lee R, Boyle WJ. Osteoprotegerin: a novel secreted protein involved in the regulation of bone density. *Cell* 1997; 89: 309-19.

Sirbu A, Kerr G, Crane M, Ruskin HJ. RNA-Seq vs dual- and single-channel microarray data: sensitivity analysis for differential expression and clustering. *PLoS One* 2012; 7: e50986.

Sodek J, Ganss B, McKee MD. Osteopontin. *Crit Rev Oral Biol Med* 2000; 11: 279-303.

Sommerfeldt DW, Rubin CT. Biology of bone and how it orchestrates the form and function of the skeleton. *Eur Spine J* 2001; 10 Suppl 2: S86-95.

Stanton LW. Methods to profile gene expression. *Trends Cardiovasc Med* 2001; 11: 49-54.

Sun H, Dai K, Tang T, Zhang X. Regulation of osteoblast differentiation by slit2 in osteoblastic cells. *Cells Tissues Organs* 2009; 190: 69-80.

Sundaram K, Nishimura R, Senn J, Youssef RF, London SD, Reddy SV. RANK ligand signaling modulates the matrix metalloproteinase-9 gene expression during osteoclast differentiation. *Exp Cell Res* 2007; 313: 168-78.

Svedbom A, Hernlund E, Ivergard M, Compston J, Cooper C, Stenmark J, McCloskey EV, Jonsson B, Kanis JA. Osteoporosis in the European Union: a compendium of country-specific reports. *Arch Osteoporos* 2013; 8: 137.

Swarthout JT, D'Alonzo RC, Selvamurugan N, Partridge NC. Parathyroid hormone-dependent signaling pathways regulating genes in bone cells. *Gene* 2002; 282: 1-17.

Teitelbaum SL. Bone resorption by osteoclasts. *Science* 2000; 289: 1504-8.

Teitelbaum SL, Ross FP. Genetic regulation of osteoclast development and function. *Nat Rev Genet* 2003; 4: 638-49.

Tella SH, Gallagher JC. Prevention and treatment of postmenopausal osteoporosis. *J Steroid Biochem Mol Biol* 2013;

Threadgill DW, Dlugosz AA, Hansen LA, Tennenbaum T, Lichti U, Yee D, LaMantia C, Mourton T, Herrup K, Harris RC, et al. Targeted disruption of mouse EGF receptor: effect of genetic background on mutant phenotype. *Science* 1995; 269: 230-4.

Titorencu I, Pruna V, Jinga VV, Simionescu M. Osteoblast ontogeny and implications for bone pathology: an overview. *Cell Tissue Res* 2013;

Tsai CL, Chen WC, Hsieh HL, Chi PL, Hsiao LD, Yang CM. TNF-alpha induces matrix metalloproteinase-9-dependent soluble intercellular adhesion molecule-1 release via TRAF2-mediated MAPKs and NF-kappaB activation in osteoblast-like MC3T3-E1 cells. *J Biomed Sci* 2014; 21: 12.

Tzahar E, Waterman H, Chen X, Levkowitz G, Karunakaran D, Lavi S, Ratzkin BJ, Yarden Y. A hierarchical network of interreceptor interactions determines signal transduction by Neu differentiation factor/neuregulin and epidermal growth factor. *Mol Cell Biol* 1996; 16: 5276-87.

Udagawa N, Takahashi N, Akatsu T, Tanaka H, Sasaki T, Nishihara T, Koga T, Martin TJ, Suda T. Origin of osteoclasts: mature monocytes and macrophages are capable of differentiating into osteoclasts under a suitable microenvironment prepared by bone marrow-derived stromal cells. *Proc Natl Acad Sci U S A* 1990; 87: 7260-4.

Villarroel-Campos D, Gonzalez-Billault C. The MAP1B case: An old MAP that is

new again. *Dev Neurobiol* 2014;

Wang Z, Gerstein M, Snyder M. RNA-Seq: a revolutionary tool for transcriptomics. *Nat Rev Genet* 2009; 10: 57-63.

Westendorf JJ, Kahler RA, Schroeder TM. Wnt signaling in osteoblasts and bone diseases. *Gene* 2004; 341: 19-39.

Wong ML, Medrano JF. Real-time PCR for mRNA quantitation. *Biotechniques* 2005; 39: 75-85.

Xian CJ. Roles of epidermal growth factor family in the regulation of postnatal somatic growth. *Endocr Rev* 2007; 28: 284-96.

Yagi M, Miyamoto T, Sawatani Y, Iwamoto K, Hosogane N, Fujita N, Morita K, Ninomiya K, Suzuki T, Miyamoto K, Oike Y, Takeya M, Toyama Y, Suda T. DC-STAMP is essential for cell-cell fusion in osteoclasts and foreign body giant cells. *J Exp Med* 2005; 202: 345-51.

Yarden Y, Sliwkowski MX. Untangling the ErbB signalling network. *Nat Rev Mol Cell Biol* 2001; 2: 127-37.

Yarden Y, Shilo BZ. SnapShot: EGFR signaling pathway. *Cell* 2007; 131: 1018.

Zhou X, Cui Y, Zhou X, Han J. Phosphate/pyrophosphate and MV-related proteins in mineralisation: discoveries from mouse models. *Int J Biol Sci* 2012; 8: 778-90.

Zhu J, Jia X, Xiao G, Kang Y, Partridge NC, Qin L. EGF-like ligands stimulate osteoclastogenesis by regulating expression of osteoclast regulatory factors by osteoblasts: implications for osteolytic bone metastases. *J Biol Chem* 2007; 282: 26656-64.

Zhu J, Shimizu E, Zhang X, Partridge NC, Qin L. EGFR signaling suppresses

osteoblast differentiation and inhibits expression of master osteoblastic transcription factors Runx2 and Osterix. *J Cell Biochem* 2011; 112: 1749-60.

IX. ADDENDUM

1. List of tables

<i>Table 1: Weighs of mice at the different ages.</i>	28
<i>Table 2: Results of Nanodrop measurement</i>	29
<i>Table 3: DAVID – selected Functional Annotation Cluster-results for 1 week group, up-regulated genes</i>	35
<i>Table 4: Gene List to Annotation terms for 1 week group, up-regulated genes</i> ...	36
<i>Table 5: Genes corresponding to biological processes for 1 week group, up-regulated genes</i>	37
<i>Table 6: DAVID – selected Functional Annotation Cluster-results for 1 week group, down-regulated genes</i>	38
<i>Table 7: Gene List to Annotation terms for 1 week group, down-regulated genes</i>	38
<i>Table 8: Genes corresponding to biological processes for 1 week group, down-regulated genes</i>	40
<i>Table 9: DAVID – selected Functional Annotation Cluster-results for 4 weeks group, up-regulated genes</i>	41
<i>Table 10: Gene List to Annotation terms for 4 weeks group, up-regulated genes</i>	41
<i>Table 11: Genes corresponding to biological processes for 4 weeks group, up-regulated genes</i>	43

2. List of figures

<i>Figure 1: Overview of the EGFR system</i>	7
<i>Figure 2: Effect of EGFR network on bone cells</i>	10
<i>Figure 3: Microarray analysis scheme</i>	12
<i>Figure 4: Hybridization process of probe with microarray chip</i>	22
<i>Figure 5: μCT analysis of distal femur</i>	26
<i>Figure 6: Example for PCR analysis</i>	27
<i>Figure 7: RNA quality analysis on agarose gel</i>	30
<i>Figure 8: Gel-like image of RNA-analysis with Bioanalyzer</i>	30
<i>Figure 9: Example for RIN-quality analysis with the Bioanalyzer</i>	31

<i>Figure 10: Heatmaps</i>	32
<i>Figure 11: Sota-cluster analysis</i>	33
<i>Figure 12: Cytoscape diagram of 1 week group, up-regulated genes</i>	37
<i>Figure 13: Cytoscape diagram of 1 week group, down-regulated genes</i>	39
<i>Figure 14: Cytoscape diagram of 4 weeks group, up-regulated genes</i>	42
<i>Figure 15: Results of qRT-PCR</i>	44

3. Primer sequences

3.1. PCR primer sequences

Areg Xba#1: 5` -TAG TCT AGA TTG CTG CAG AGA CCG AGA C -3`

Areg Pac#2: 5` -TAG TTA ATT AAG GCA ATG ATT CAA CTT TTA CC -3`

Errb2 fl up: 5` -TTT ATG TGG GCA CGC TTA GAA C- 3`

Erb2 fl lw: 5` -CTA GAA GTC TGA TTT GCG GTA T- 3`

3.2. qRT-PCR primer sequences

mMMP9_1992_FW: 3` CGT CAT TCG CGT GGA TAA GG 5`

mMMP9_2110_RV: 3` TTT GGA AAC TCA CAC GCC AG 5`

mRANKL_673_FW: 3` GAA ACA TCG GGA AGC GTA CC 5`

mRANKL_782_RV: 3` TTC GTG CTC CCT CCT TTC AT 5`

mOPG_488_FW: 3` ACA CGA ACT GCA GCA CAT TT 5`

mOPG_582_RV: 3` CTT TTG CGT GGC TTC TCT 5`

mDCSTAMP_978_FW: 3` ACA GTT CCA AAG CTT GCC AG 5`

mDCSTAMP_1106_RV: 3` GGT TTA GGA ATG CAG CTC GG 5`

house keeping gene:

mGAPDH_FW : 3` TCATCAACGGGAAGCCCATCAC 5`

mGAPDH_RV: 3` AGACTCCACGACATACTCAGCACCG 5`

4. List of genes

4.1. 1 week, differentially expressed up-regulated genes

Gene Number	Gene Symbol	Gene Name	Fold Change	Adjusted p-value
NM_009704	Areg	Amphiregulin	207,074	0,000
NM_029838	Col25a1	collagen, type XXV, alpha 1	3,514	0,005
NM_010054	Dlx2	distal-less homeobox 2	3,317	0,007
NM_009263	Spp1	secreted phosphoprotein 1 = Osteopontin	3,143	0,007
NM_007670	Cdkn2b	cyclin-dependent kinase inhibitor 2B	3,091	0,005
ENSMUST00000105520	Enpp1	ectonucleotide pyrophosphatase/phosphodiesterase 1	2,942	0,005
NM_009877	Cdkn2a	cyclin-dependent kinase inhibitor 2A	2,868	0,007
NM_019950	Chst5	carbohydrate (N-acetylglucosamine 6-O) sulfotransferase 5	2,868	0,007
NM_011670	Uchl1	ubiquitin carboxy-terminal hydrolase L1	2,774	0,005
NM_198711	Col25a1	collagen, type XXV, alpha 1 transcript variant 2	2,556	0,005
NM_008815	Etv4	ets variant gene 4 (E1A enhancer binding protein, E1AF)	2,533	0,007
NM_018857	Msln	mesothelin	2,504	0,005
NM_008634	Map1b	microtubule-associated protein 1B	2,469	0,007
NM_028325	Zcchc12	zinc finger, CCHC domain containing 12	2,457	0,007
NM_001001979	Megf10	multiple EGF-like-domains 10	2,445	0,005
NM_008813	Enpp1	ectonucleotide pyrophosphatase/phosphodiesterase 1	2,428	0,007
NM_008872	Plat	plasminogen activator, tissue	2,385	0,008
NM_008926	Prkg2	protein kinase, cGMP-dependent, type II	2,344	0,007
chr5:152006587-152008784_R		n.c. (non coding)	2,264	0,007
chr5:152006587-152008784_R		n.c.	2,263	0,005
NM_009115	S100b	S100 protein, beta polypeptide, neural	2,247	0,009
chr5:152006587-152008784_R		n.c.	2,219	0,007
NM_010181	Fbn2	fibrillin 2	2,198	0,007
NM_153800	Arhgap22	Rho GTPase activating protein 22	2,167	0,007
NM_013599	Mmp9	matrix metalloproteinase 9	2,157	0,007
NM_029770	Unc5b	unc-5 homolog B (C. elegans)	2,151	0,007
chr5:14943275-14944205_F		n.c.	2,149	0,019
NM_024474	Col26a1	collagen, type XXVI, alpha 1	2,149	0,008
NM_008815	Etv4	ets variant gene 4 (E1A enhancer binding protein, E1AF)	2,145	0,018
NM_178804	Slit2	slit homolog 2 (Drosophila)	2,139	0,007
NM_026838	Srpx2	sushi-repeat-containing protein, X-linked 2, transcript variant 1	2,123	0,007
NM_029422	Dcstamp	dendrocyte expressed seven transmembrane protein	2,086	0,007
NM_173770	Fam69c	family with sequence similarity 69, member C	2,082	0,007
NM_001044384	Timp1	tissue inhibitor of metalloproteinase 1, transcript variant 1	2,071	0,005
chr5:15146475-15170100_F		n.c.	2,069	0,037
NM_015755	Hunk	hormonally upregulated Neu-associated kinase	2,062	0,007
NM_008100	Gcg	glucagon	2,048	0,007

Gene Number	Gene Symbol	Gene Name	Fold Change	Adjusted p-value
chr5:15146475-15170100_F		n.c.	2,041	0,019
NM_010181	Fbn2	fibrillin 2	2,032	0,007
NM_009324	Tbx2	T-box 2	2,027	0,008
chr13:56851404-56851796_R		n.c.	2,021	0,019
chr13:56851404-56851796_R		n.c.	2,018	0,007
NM_001164763	Rarres1	retinoic acid receptor responder (tazarotene induced) 1	2,013	0,007
NM_172864	Wdr63	WD repeat domain 63	2,013	0,008
NM_010373	Gzme	granzyme E	2,010	0,011
NM_010737	Klrb1a	killer cell lectin-like receptor subfamily B member 1A, transcript variant 1	2,007	0,011
NM_028775	Cyp2s1	cytochrome P450, family 2, subfamily s, polypeptide 1	2,007	0,007
AK019926		adult male pituitary gland cDNA, RIKEN full-length enriched library	2,006	0,008

4.2. 1 week, differentially expressed, down-regulated genes

Gene Number	Gene Symbol	Gene Name	Fold Change	Adjusted p-value
NM_010815	Grap2	GRB2-related adaptor protein 2	0,500	0,010
chr10:69819062-69871640_F		n.c.	0,500	0,009
NM_152823	Unc5cl	unc-5 homolog C (C. elegans)-like	0,500	0,026
chr2:153325670-153352170_R		n.c.	0,499	0,048
A_55_P1958902		n.c.	0,499	0,007
chr16:89961600-89971725_R		n.c.	0,498	0,007
NM_007998	Fech	ferrochelatase	0,498	0,007
NM_172577	Slc25a21	solute carrier family 25 (mitochondrial oxodicarboxylate carrier), member 21, transcript variant 1	0,498	0,007
NM_011465	Spta1	spectrin alpha, erythrocytic 1	0,498	0,007
NM_011527	Tal1	T cell acute lymphocytic leukemia 1	0,498	0,008
AK048886		0 day neonate cerebellum cDNA	0,497	0,011
NM_008185	Gstt1	glutathione S-transferase, theta 1	0,497	0,007
NM_022986	lrak1bp1	interleukin-1 receptor-associated kinase 1 binding protein 1, transcript variant 1	0,497	0,011
chr15:84737071-84744158_F		n.c.	0,497	0,020
NM_009479	Uros	uroporphyrinogen III synthase	0,497	0,007
XM_621386	Gm5958	predicted pseudogene 5958	0,497	0,010
NM_139303	Kif18a	kinesin family member 18A	0,496	0,007
NM_001142952	Fam46c	family with sequence similarity 46, member C	0,496	0,009
NM_029264	Ttl10	tubulin tyrosine ligase-like family, member 10	0,496	0,007
ENSMUST00000103526	Ighv1-55-201	immunoglobulin heavy variable 1-55	0,495	0,030
chr5:77084398-77086144_R		n.c.	0,495	0,007
NM_001081349	Slc43a1	solute carrier family 43, member 1 (Slc43a1), transcript variant 1	0,495	0,008

ENSMUST00000111637	Ube2l6-202	ubiquitin-conjugating enzyme E2L 6 Gene	0,494	0,007
chr8:83210957-83219451_F		n.c.	0,494	0,007
NM_183173	Sowaha	sosondowah ankyrin repeat domain family member A	0,494	0,007
ENSMUST00000045307		n.c.	0,494	0,010
NM_001033286	Slc30a10	solute carrier family 30, member 10	0,494	0,018
NM_001008499	Taar4	trace amine-associated receptor 4	0,493	0,044
NM_001013784	E130309D14Rik	RIKEN cDNA E130309D14 gene	0,492	0,009
NM_177733	E2f2	E2F transcription factor 2	0,491	0,007
NM_008135	Slc6a9	solute carrier family 6 (neurotransmitter transporter, glycine), member 9	0,491	0,008
NM_011722	Dctn6	dynactin 6	0,491	0,007
NM_026331	Slc25a37	solute carrier family 25, member 37	0,491	0,008
NM_138955	Abcg4	ATP-binding cassette, sub-family G (WHITE), member 4	0,491	0,010
NM_001177731	Mrap2	melanocortin 2 receptor accessory protein 2 (Mrap2), transcript variant 1	0,491	0,024
ENSMUST00000103469	Ighv14-3-001	immunoglobulin heavy variable V14-3	0,491	0,010
ENSMUST00000050753		Transcript: A930002H24Rik-201	0,490	0,040
NM_031880	Tnk1	tyrosine kinase, non-receptor, 1	0,490	0,007
NM_134021	Pnpo	pyridoxine 5'-phosphate oxidase	0,490	0,007
NM_001159626	Hagh	hydroxyacyl glutathione hydrolase (Hagh), transcript variant 2	0,490	0,008
NM_011270	Rhd	Rh blood group, D antigen	0,489	0,007
chr6:052032838-052033444		n.c.	0,489	0,031
NM_011269	Rhag	Rhesus blood group-associated A glycoprotein	0,489	0,008
NM_144533	Nmnat3	nicotinamide nucleotide adenyltransferase 3	0,489	0,007
NM_007570	Btg2	B cell translocation gene 2, anti-proliferative	0,489	0,008
NM_008114	Gfi1b	growth factor independent 1B, transcript variant 1	0,488	0,007
NM_025912	Fam210b	family with sequence similarity 210, member B	0,488	0,008
XM_003086781		n.c.	0,488	0,015
BC003861	cDNA clone MGC:6604 IMAGE:3487642	hydroxymethylbilane synthase, mRNA (cDNA clone MGC:6604 IMAGE:3487642), complete cds	0,488	0,009
NM_029964	6030468B19Rik	RIKEN cDNA 6030468B19 gene	0,488	0,007
NM_009514	Vpreb3	pre-B lymphocyte gene 3	0,488	0,008
NM_144869	BC021614	cDNA sequence BC021614	0,487	0,011
NM_001029872	Itgad	integrin, alpha D	0,487	0,013
chr4:155585650-155608700_R		n.c.	0,487	0,016
NM_019687	Slc22a4	solute carrier family 22 (organic cation transporter), member 4	0,486	0,007
ENSMUST00000022711		RIKEN cDNA 4930449E01 gene	0,485	0,008
ENSMUST00000065159		n.c.	0,484	0,009
ENSMUST00000103537	Ighv1	immunoglobulin heavy variable 1-66	0,484	0,021
NM_027464	Fam213a	family with sequence similarity 213, member A	0,484	0,007
NM_008102	Gch1	GTP cyclohydrolase 1	0,483	0,007
A_55_P1976450		n.c.	0,483	0,021

ENSMUST00000103410	Igkc	immunoglobulin kappa constant	0,483	0,046
NM_001038699	Fn3k	fructosamine 3 kinase, transcript variant 2	0,483	0,019
NM_020583	Isg20	interferon-stimulated protein, transcript variant 1	0,483	0,007
ENSMUST00000107465		n.c.	0,482	0,009
NM_008089	Gata1	GATA binding protein 1	0,482	0,008
NM_001013368	E2f8	E2F transcription factor 8	0,481	0,009
NM_011638	Tfrc	transferrin receptor	0,481	0,007
NM_146173	Tspan33	tetraspanin 33	0,481	0,007
chr9:40029344-40050160_F		n.c.	0,479	0,018
NM_009653	Alas2	aminolevulinic acid synthase 2, erythroid (Alas2), transcript variant 1	0,479	0,008
XR_105911		Redrum, erythroid developmental long intergenic non-protein coding transcript (Redrum), non-coding RNA	0,479	0,008
NM_009345	Dntt	deoxynucleotidyltransferase, terminal, transcript variant 1	0,477	0,013
chr8:122807653-122823000_R		n.c.	0,476	0,014
NM_197999	Ces2g	carboxylesterase 2G	0,476	0,007
NM_001177416	Gm6792	predicted gene 6792, transcript variant 1	0,476	0,008
chr6:145936225-145965575_F		n.c.	0,475	0,007
chr13:81773237-81783062_F		n.c.	0,474	0,007
NM_011403	Slc4a1	solute carrier family 4 (anion exchanger), member 1	0,474	0,008
chr2:118408095-118415745_F		n.c.	0,473	0,012
NM_009699	Aqp2	aquaporin 2	0,473	0,024
NM_026527	Chac2	ChaC, cation transport regulator 2	0,472	0,007
NM_146010	Tspan8	tetraspanin 8 (Tspan8), transcript variant 1	0,471	0,007
NM_001110320	Cd72	CD72 antigen (Cd72), transcript variant 1	0,471	0,009
NM_013514	Dmtn	dematin actin binding protein (Dmtn), transcript variant 2	0,470	0,007
NM_009973	Csn1s2b	casein alpha s2-like B	0,470	0,008
AK020830		adult retina cDNA, RIKEN full-length enriched library, clone:A930008G19 product:HYPOTHETICAL PROTEIN KIAA0140 homolog [Homo sapiens], full insert sequence	0,470	0,007
chr10:66349796-66378261_R		n.c.	0,469	0,017
chr5:35893909-35899497_R		n.c.	0,468	0,007
chr9:89167172-89168980_F		n.c.	0,467	0,012
NM_010635	Klf1	Kruppel-like factor 1 (erythroid)	0,467	0,011
NM_001033301	Fhdc1	FH2 domain containing 1, transcript variant 2	0,467	0,009
NM_010149	Epore	erythropoietin receptor	0,467	0,007
NM_001164557	Pdzk1ip1	PDZK1 interacting protein 1, transcript variant 1	0,467	0,009
NM_001195094	Ccdc42b	coiled-coil domain containing 42B	0,467	0,014
NM_001037634	Oosp2	oocyte secreted protein 2	0,466	0,007
ENSMUST00000109709		RIKEN cDNA 1700003F12 gene	0,464	0,008
NM_020583	Isg20	interferon-stimulated protein, transcript variant 1	0,464	0,007

NM_172479	Slc38a5	solute carrier family 38, member 5	0,464	0,008
NM_001042451	Snca	synuclein, alpha (Snca), transcript variant 1	0,463	0,007
AK047639		adult male corpus striatum cDNA, RIKEN full-length	0,463	0,008
NM_001199971	Tac2	tachykinin 2, transcript variant 2	0,463	0,026
NM_007799	Ctse	cathepsin E	0,463	0,007
NM_020504	Cldn13	claudin 13	0,462	0,009
NM_175000	Hbq1a	hemoglobin, theta 1A	0,460	0,007
NM_177564	Dhrs11	dehydrogenase/reductase (SDR family) member 11	0,460	0,012
NM_001167746	Dnah17	dynein, axonemal, heavy chain 17	0,459	0,009
chr12:32781477-32808567_R		n.c.	0,458	0,007
NM_145981	Phyhip	phytanoyl-CoA hydroxylase interacting protein	0,457	0,017
NM_001131020	Gfap	glial fibrillary acidic protein (Gfap), transcript variant 1	0,456	0,008
XM_003085972	Gm10362	predicted gene 10362	0,456	0,031
NM_023892	Icam4	intercellular adhesion molecule 4, Landsteiner-Wiener blood group	0,455	0,009
NM_030069	Nxpe2	neurexophilin and PC-esterase domain family, member 2	0,455	0,007
NM_178667	Tfdp2	transcription factor Dp 2, transcript variant 1	0,455	0,007
chr5:149765314-149771786_R		n.c.	0,454	0,007
chr15:101084597-101095097_F		n.c.	0,453	0,007
NM_172709	Otop1	otopetrin 1	0,453	0,007
chr12:32781477-32808567_R		n.c.	0,452	0,008
NM_178715	Tmem30b	transmembrane protein 30B	0,452	0,009
NM_027600	4921504E06Rik	RIKEN cDNA 4921504E06 gene	0,452	0,014
NM_011465	Spta1	spectrin alpha, erythrocytic 1	0,452	0,007
XM_356935		n.c.	0,450	0,007
NM_028025	Mageb16	melanoma antigen family B, 16, transcript variant 1	0,450	0,008
NM_032540	Kel	Kell blood group	0,449	0,007
NM_013848	Ermap	erythroblast membrane-associated protein	0,449	0,008
chr5:122982442-123000053_F		n.c.	0,449	0,007
ENSMUST00000152722	Sult5a1	sulfotransferase family 5A, member 1	0,448	0,008
NM_001164557	Pdzk1ip1	PDZK1 interacting protein 1, transcript variant 1	0,448	0,008
NM_011312	S100a5	S100 calcium binding protein A5	0,446	0,009
NM_138678	Btnl10	butyrophilin-like 10	0,445	0,008
ENSMUST00000034133	Mylk3	myosin light chain kinase 3	0,445	0,005
XR_105468	5430401H09Rik	n.c.	0,444	0,008
XR_106478		n.c.	0,440	0,014
NM_011280	Trim10	tripartite motif-containing 10	0,437	0,007
NM_022014	Fn3k	fructosamine 3 kinase, transcript variant 1	0,437	0,007
NM_013848	Ermap	erythroblast membrane-associated protein	0,436	0,008
chr12:32781477-32808567_R		n.c.	0,434	0,008
chr15:85412264-85549139_F		n.c.	0,433	0,018

NM_016975	Gja3	gap junction protein, alpha 3, transcript variant 1	0,433	0,022
NM_175684	Fchsd1	FCH and double SH3 domains 1	0,431	0,009
NM_019991	Prl2a1	prolactin family 2, subfamily a, member 1	0,430	0,015
NM_023117	Cdc25b	cell division cycle 25B, transcript variant 1	0,428	0,008
NM_013513	Epb4.2	erythrocyte protein band 4.2	0,427	0,007
NM_026875	Ypel3	yippee-like 3 (Drosophila)	0,426	0,008
chr17:22420025-22457650_F		n.c.	0,425	0,012
NM_001080943	Zdhc22	zinc finger, DHHC-type containing 22	0,425	0,007
NM_001033981	Hbq1b	hemoglobin, theta 1B	0,423	0,006
NM_013467	Aldh1a1	aldehyde dehydrogenase family 1, subfamily A1	0,421	0,010
NM_011439	Sox13	SRY-box containing gene 13	0,417	0,009
NR_033575	Gm12839	predicted gene 12839, non-coding RNA	0,416	0,009
NM_019866	Spib	Spi-B transcription factor (Spi-1/PU.1 related)	0,415	0,012
ENSMUST00000109705		n.c.	0,412	0,014
NM_027918	1300017J02Rik	RIKEN cDNA 1300017J02 gene	0,410	0,008
NM_010369	Gypa	glycophorin A	0,407	0,007
NM_145141	Fcrla	Fc receptor-like A	0,404	0,013
A_55_P2028214		n.c.	0,404	0,007
NM_001034866	Pnlcd1	poly(A)-specific ribonuclease (PARN)-like domain containing 1	0,402	0,046
NM_026132	Txndc8	thioredoxin domain containing 8	0,400	0,038
NM_001174086	Shisa9	shisa homolog 9 (Xenopus laevis), transcript variant 2	0,397	0,033
chr2:77146893-77155643_F		n.c.	0,384	0,005
chr11:69185658-69186082_F		n.c.	0,384	0,017
chr8:106037800-106070025_F		n.c.	0,382	0,008
chr1:36086491-36087863_R		n.c.	0,380	0,007
ENSMUST00000124863		n.c.	0,379	0,009
NM_139142	Slc6a20a	solute carrier family 6 (neurotransmitter transporter), member 20A	0,373	0,007
NM_001127354	Gm11938	predicted gene 11938	0,372	0,009
NM_030180	Usp54	ubiquitin specific peptidase 54	0,362	0,009
NM_001011749	Olfir704	olfactory receptor 704	0,360	0,010
ENSMUST00000101091		n.c.	0,356	0,007
NM_027802	Obox1	oocyte specific homeobox 1	0,355	0,033
chr12:5303823-5379098_R		n.c.	0,354	0,014
NM_008102	Gch1	GTP cyclohydrolase 1	0,347	0,007
NM_001109985	Nos1ap	nitric oxide synthase 1 (neuronal) adaptor protein, transcript variant 1	0,331	0,007
ENSMUST00000132717	Mbd5	methyl-CpG binding domain protein 5	0,328	0,007
chr8:94841965-94881130_R		n.c.	0,320	0,008
NR_015605	2900052N01Rik	RIKEN cDNA 2900052N01 gene (2900052N01Rik), long non-coding RNA	0,311	0,011
chr10:60473030-60535340_R		n.c.	0,311	0,012
chr9:96635508-96654148_R		n.c.	0,308	0,010
NM_001146351	Ephb6	Eph receptor B6, transcript variant 1	0,308	0,010

chr9:31834945-32015745_R		n.c.	0,304	0,009
chrX:20570399-20571162_F		n.c.	0,298	0,008
NAP092838-001		n.c.	0,288	0,009
ENSMUST00000108646		n.c.	0,252	0,008
TC1683061		Very low-density lipoprotein receptor variant (Fragment), partial (7%) [TC1683061]	0,166	0,007

4.3. 4 weeks, differentially expressed up-regulated genes

Gene Number	Gene Symbol	Gene Name	Fold Change	Adjusted p-value
NM_009704	Areg	Amphiregulin	94,092	0,000
NM_009877	Cdkn2a	cyclin-dependent kinase inhibitor 2A	3,329	0,003
NM_018857	Msln	mesothelin	2,965	0,003
NM_029838	Col25a1	collagen, type XXV, alpha 1	2,674	0,003
NM_007670	Cdkn2b	cyclin-dependent kinase inhibitor 2B (p15, inhibits CDK4)	2,650	0,003
NM_009263	Spp1	secreted phosphoprotein 1	2,610	0,003
NM_001001979	Megf10	multiple EGF-like-domains 10	2,603	0,003
NM_010180	Fbln1	fibulin 1	2,497	0,003
NM_008634	Map1b	microtubule-associated protein 1B	2,464	0,003
NM_019950	Chst5	carbohydrate (N-acetylglucosamine 6-O) sulfotransferase 5	2,445	0,003
NM_010181	Fbn2	fibrillin 2	2,393	0,008
NM_008481	Lama2	laminin, alpha 2	2,383	0,008
NM_033592	Pcdhga9	protocadherin gamma subfamily A, 9	2,320	0,003
ENSMUST00000105520	Enpp1	ectonucleotide pyrophosphatase/phosphodiesterase 1	2,291	0,003
NM_008481	Lama2	laminin, alpha 2	2,245	0,021
NM_010181	Fbn2	fibrillin 2	2,221	0,004
NM_001044384	Timp1	tissue inhibitor of metalloproteinase 1	2,219	0,003
NM_008872	Plat	plasminogen activator, tissue	2,213	0,008
NM_053110	Gpnmb	glycoprotein (transmembrane) nmb	2,207	0,003
NM_178804	Slit2	slit homolog 2	2,186	0,003
NM_007739	Col8a1	collagen, type VIII, alpha 1	2,161	0,005
AI428898	mp51g11.x1	n.c. (non coding)	2,158	0,003
NM_138686	Cys1	cystin 1	2,145	0,044
NM_010140	Epha3	Eph receptor A3	2,145	0,003
NM_026838	Srpx2	sushi-repeat-containing protein, X-linked 2	2,144	0,003
AK009210		unclassifiable, full insert sequence	2,133	0,007
NM_176954	Celf5	CUGBP, Elav-like family member 5	2,132	0,004
chr19:5834117-5835940_R		n.c.	2,127	0,004
NM_011670	Uchl1	ubiquitin carboxy-terminal hydrolase L1	2,111	0,009
AK048087		unclassifiable, full insert sequence	2,104	0,027
NM_009116	Prrx2	paired related homeobox 2	2,101	0,018
NM_010171	F3	coagulation factor III	2,095	0,003
NM_011607	Tnc	tenascin C	2,082	0,003
chr5:152006587-152008784_R		n.c.	2,081	0,003
chr5:152006587-152008784_R		n.c.	2,076	0,003
NM_198711	Col25a1	collagen, type XXV, alpha 1	2,075	0,003
NM_177588	Thnsl1	threonine synthase-like 1	2,073	0,015
NM_175499	Slitrk6	SLIT and NTRK-like family, member 6	2,071	0,004

Gene Number	Gene Symbol	Gene Name	Fold Change	Adjusted p-value
NM_001043355	Map6	microtubule-associated protein 6	2,065	0,008
A_55_P2041693		n.c.	2,065	0,003
NM_175686	Prrx1	paired related homeobox 1	2,065	0,003
BX527063		n.c.	2,063	0,003
NM_001081407	Plb1	phospholipase B1	2,062	0,003
AK084291		unclassifiable, full insert sequence	2,061	0,036
NM_001177574	Gm2022	predicted pseudogene 2022	2,059	0,005
NM_016919	Col5a3	collagen, type V, alpha 3	2,055	0,012
NM_001177573		n.c.	2,046	0,005
NM_007899	Ecm1	extracellular matrix protein 1	2,041	0,005
DV650784		n.c.	2,039	0,007
chr5:152006587-152008784_R		n.c.	2,032	0,006
NM_011607	Tnc	tenascin C	2,025	0,006
NM_027602	Nsun7	NOL1/NOP2/Sun domain family, member 7	2,020	0,004
chr19:5834117-5835940_R		n.c.	2,015	0,006
chr4:128727332-128735227_F		n.c.	2,015	0,007
NM_009866	Cdh11	cadherin 11	2,014	0,004
NM_007899	Ecm1	extracellular matrix protein 1	2,011	0,003
NM_028775	Cyp2s1	Mus musculus cytochrome P450, family 2, subfamily s, polypeptide 1	2,004	0,005

4.4. 4 weeks, differentially expressed down-regulated genes

Gene Number	Gene Symbol	Gene Name	Fold Change	Adjusted p-value
chr5:149765314-149771786_R		n.c.	0,483	0,006
NM_016982	Vpreb1	Mus musculus pre-B lymphocyte gene 1	0,434	0,004
NM_001190325	Igll1	Mus musculus immunoglobulin lambda-like polypeptide 1	0,427	0,003
NM_009246	Serpina1d	serine (or cysteine) peptidase inhibitor, clade A, member 1D	0,478	0,011
NM_009245	Serpina1c	serine (or cysteine) peptidase inhibitor, clade A, member 1C	0,452	0,009
A_55_P2046709		n.c.	0,474	0,011
NM_009247	Serpina1e	serine (or cysteine) peptidase inhibitor, clade A, member 1E	0,465	0,013
NM_009243	Serpina1a	serine (or cysteine) peptidase inhibitor, clade A, member 1A	0,463	0,014

X. ACKNOWLEDGMENT

First of all I would like to thank my *Doktorvater* PD Dr. Marlon Schneider for providing me with this work, for all his help and guidance, and for his almost constant availability for questions of all kinds.

I am indebted to Prof. Eckart Wolf for the ability, to carry out this work at the Institute for Molecular Animal Breeding and Biotechnology, Gene Center.

Many thanks to the working group of Dr. Helmut Blum for conducting the microarray experiments and also their help with all the questions I had; here are to mention Dr. Helmut Blum, Alexander Graf, Andrea Klanner, Dr. Stefan Krebs and Sylvia Mallok.

To all my dear colleagues, Dr. Felix Hiltwein, Franziska Stumpf, Freya Jay, Dr. Mai Le, Sepp Millauer, Stefanie Riesemann, Dr. Maik Dahlhoff and Tamara Holy, many, many thanks, for introducing me to laboratory work, for help of all kinds, especially during my pregnancies, and of course for the fun!

Special thanks to Dr. Jessica Grill for her help and for arranging qRT-PCR analysis, and I would also like to thank Andrea Ofner and PD Dr. Andreas Herbst for their great help.

To Dr. Ingrid Renner-Müller for her guidance and help, especially with all the questions around animal study proposals and for regular provision with sweets many thanks. Many thanks also to Petra Renner, Insa Buchacz, and all the former and present colleagues of the animal facility team for excellent animal maintenance.

Special thanks to secretary Sylvia Hornig for all the necessary paper work and of course her commitment in all social affairs, especially daily lunch planning.

To my beloved family many thanks for all your priceless help.